

International

WOCE

Newsletter



Number 18

March 1995

IN THIS ISSUE

	page
<input type="checkbox"/> From the IPO	
1995 - A Turning Point for WOCE <i>W.J. Gould</i>	2
<input type="checkbox"/> Science	
Meridional Volume and Heat Transport in the Pacific Sector of the Antarctic <i>M.N. Koshlyakov and T.G. Sazhina</i>	3
The Weddell Gyre Study 1989 - 1993 <i>E. Fahrbach, G. Rohardt, M. Schröder and V. Strass</i>	6
Bottom Water Anomaly at the Subantarctic Front on Greenwich Meridion <i>M. Schröder, M. Hoppema and A. Wisotzki</i>	10
Carbon Dioxide Investigations During the Weddell Gyre Study <i>M. Hoppema and E. Fahrbach</i>	12
Comparing WOCE and Historical Temperatures in the Deep Southeast Pacific <i>J. Swift</i>	15
WOCE Observations in the Southern Ocean <i>N.P. Holliday</i>	18
OCCAM: the Ocean Circulation and Climate Advanced Modelling Project <i>P.D. Killworth</i>	20
Early ALACE Results from the Pacific <i>R.E. Davis</i>	22
RAFOS Floats in the Antarctic Intermediate Water of the South Atlantic <i>O. Boebel and C. Schmid</i>	26
Meridional Transport Estimates for the Northern North Atlantic <i>M. Bersch and J. Meincke</i>	28
ACSYS: The Arctic Climate System Study <i>K. Aagaard</i>	31
<input type="checkbox"/> Data Issues	
WOCE DAC/SAC for Surface Meteorology Data and Surface Flux Analysis <i>D.M. Legler</i>	32
A Consistent pre-WOCE Hydrographic Dataset for the South Atlantic: Station Data and Gridded Fields <i>V. Gouretski and K. Jancke</i>	34
WHP Manuals On-Line <i>C.E. Corry and K. Jancke</i>	37
A Note on Data Sharing Policy <i>J. Crease</i>	38
WOCE IPO Publications Since the Start of 1994	39
<input type="checkbox"/> Meetings Timetable	40

1995 – A Turning Point for WOCE

W. John Gould, Director, WOCE IPO

1995 is going to be an important year for WOCE. In many ways it marks a turning point at which WOCE will change its emphasis from one of finding the resources to carry out observations to one in which planning for and carrying out the analysis, interpretation and synthesis becomes the dominant focus.

Observations are still underway, particularly in the Indian Ocean and as I write this article we have just heard that permission has been granted for the first WOCE observations to be carried out in Indian waters. A year from now the Indian Ocean survey will be largely complete. It has taken a great deal of effort, particularly by the US WOCE Office, to ensure that these observations get done and we await its completion and with it the greater part of the global one-time survey.

Measurements on the North Atlantic have taken place since the beginning of WOCE but much remains to be done to achieve a coherent and quasi-synoptic survey of its circulation and to address many of the objectives set out in WOCE Core Project 3. A wide ranging international effort for 1996/7 in the North Atlantic has been planned over the past year. It will serve to provide a measure of the “smearing” of WOCE data over a number of years compared with data collected in a more synoptic fashion. It will also provide a baseline against which the surprisingly large subsurface temperature and salinity anomalies that WOCE has already started to document may be assessed in a more systematic way. Finally, if the resources can be found, pre- and post-winter surveys of selected sections will document the products of winter convection in the subpolar gyre. Planning was largely completed at a meeting in Atlanta in February. A report of the meeting will appear in the next Newsletter.

WOCE has presented a new set of challenges to oceanographers. WOCE made many observational oceanographers think globally about the ocean for the first time. The assembly of basin-wide, and ultimately global, data sets of uniformly high quality is a large undertaking. The first and essential step towards that goal is for individual PIs to submit their data to the WOCE Data Assembly Centres in a timely fashion. Although we have come to recognise that the timescales for data submission laid out in

the Implementation Plan were over-optimistic, we cannot allow unlimited extensions of deadlines. The DACs and SACs will be making strenuous efforts throughout 1995 to get the data. I encourage all of you who have data sets that are overdue to work with the staff of the DACs to get the data moving. Ultimately the success of WOCE depends on you individuals.

WOCE has started to prepare a strategy which will outline the steps needed to be undertaken for WOCE to move from just having a collection of observations to producing a global view of the oceans in the 1990s and with it improved ocean models. At the March 1995 meeting of our parent body, the Joint Scientific Committee for the World Climate Research Programme, WOCE will be presenting its strategy for the programme up to and beyond 1997.

WOCE SSG has already slimmed down its science infrastructure and much of the future science planning and oversight will be carried out by a new Synthesis and Modelling Working Group co-chaired by Andrew Bennett and Lynne Talley. Their WG will be charged with thinking through and defining the strategy to carry out the synthesis of WOCE results.

The WOCE SSG strongly believes that WOCE needs to continue to exist as a separate WCRP programme until the analysis, interpretation and synthesis of WOCE results are essentially complete. This, we estimate will be in 2002. In the next Newsletter I will report the results of the JSC presentation.

This issue of the Newsletter contains a number of articles on the Southern Ocean. In addition we continue the presentation of WOCE related numerical modelling efforts with an article on OCCAM by Peter Killworth. Two of our DACs/SACs report on their work and Russ Davis presents first results from ALACE floats, which were developed specially for WOCE. Andrea Frische, our Editor, has done such a good job in encouraging articles to be submitted that we have had to hold over some articles already in hand for the next Newsletter. Our strategy in future will be to have Newsletters of no more than 40 pages but to increase the publication rate to 4 issues per year. The next one will appear in June, focusing on the Pacific Ocean and reports from the latest meetings and workshops.

In our last issue we enclosed a card requesting you to confirm that you want to continue to receive the Newsletter. Thanks to all of you who replied. We now have a substantial number of new readers – however quite a few have still not replied so this is your last chance. If we don't hear from you by June you won't receive the WOCE Newsletter any more.

Meridional Volume and Heat Transport in the Pacific Sector of the Antarctic

M.N. Koshlyakov and T.G. Sazhina, P.P. Shirshov Institute of Oceanology, Russian Academy of Sciences, Moscow 117851, Russia

The work is based on the S4 Pacific section (Fig. 1) carried out by the Russian-USA expedition aboard the RV Akademik Ioffe in February-March 1992. The section, the main part of which was extended along 67°S, consisted of 115 full depth CTD/rosette stations. Current measurements by a 75 kHz ADCP, combined with the GPS, were also made. Temporal averaging of the ADCP data enabled us to obtain representative (with the mean error of 0.5 cm/s) values of the ADCP velocity, averaged over station time, at 400 m depth for the station points. The strong slope of isotherms at 125–140°W in Fig. 2 shows transition from the Ross Gyre to the Antarctic Circumpolar Current (ACC), see Fig. 1.

The typical value of the baroclinic Rossby scale for the area under study is 10 miles which is several times less than the S4 station spacing (30 or 40 miles in the open ocean). To obtain large-scale components of the temperature, salinity, density and ADCP velocity distributions in the S4 section, the mesoscale noise had to be eliminated from these fields by their smoothing along the section. The optimal smoothing scale (2200 km as the wave length, amplitude of which is diminished by $1/\sqrt{2}$ times) for the open ocean part of the S4 was found by the spatial (longitudinal) spectral analysis of these fields along this section's part. The oceanic fields within the boundary regions near the continental slope of Antarctic Peninsula at the eastern end of the S4 and of the Pennell Coast at its western end were not smoothed at all. A minimum smoothing was used for the transitional areas between the open ocean and the boundary regions.

Large-scale geostrophic currents (Fig. 3) were calculated from the smoothed density field with the smoothed ADCP velocity distribution at 400 m depth (with the mean error of 0.14 cm/s after smoothing) as reference distribution. For the western half of section 4, where ADCP measurement was absent, the velocity was calculated from the level of no motion, coinciding with the outer boundary of the cold (Fig. 2), salty and dense "spot" of the bottom water coming from the western part of the Ross Sea. Practically zero volume transport across the entire section was obtained after this procedure. To obtain exact zero, we needed only to increase by 0.03 cm/s the current velocity out of the Antarctic area (AAA) at all depths at the last eastern station of the section's part 3 (Fig. 3). We do not take into account Ekman transport because of the absence of the corresponding mean wind data for the S4 period. Closeness of S4 to the Antarctic Divergence and the very variable wind direction shipborne data support this choice.

Currents to the south at 115–160°W, to the north at 77–115°W, into the AAA across the section's part 2 and out of the AAA across the part 1 (Fig. 3) correspond well with the mean circulation pattern in this part of the Antarctic, being connected with the curvature of the ACC southern jets (Fig. 1). Volume transport of the boundary current over the continental slope of the Antarctic Peninsula is 10.2 Sv. Currents to the north-west at the lower and very upper parts of the continental slope of the Pennell Coast (Figs. 1 and 3) mark respectively the flow of the Antarctic Bottom Water from the western part of the Ross Sea with 2 Sv and the Antarctic Coastal Current with 0.2 Sv.

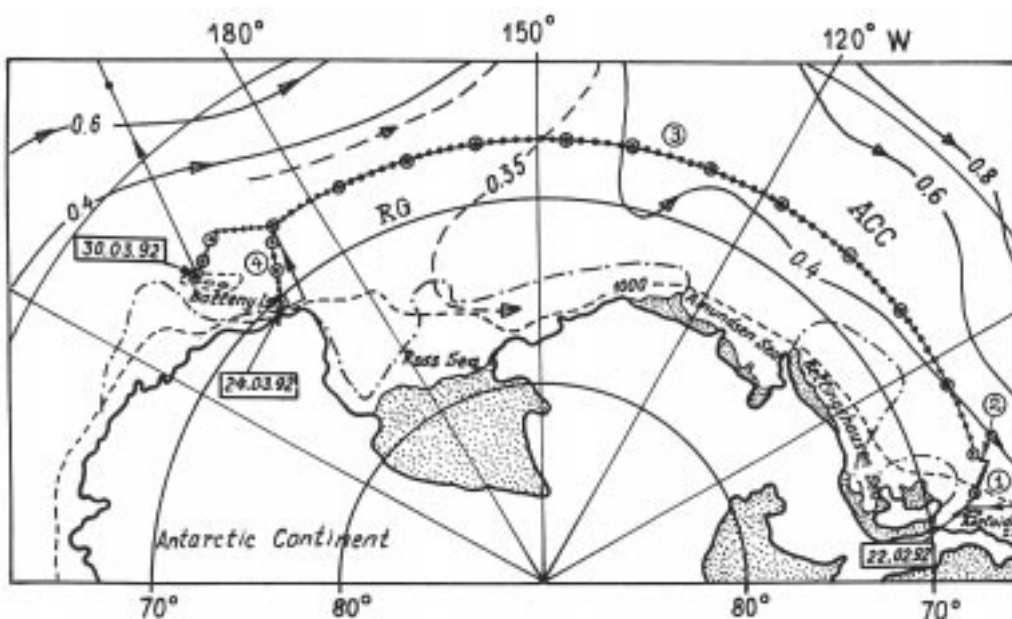


Figure 1. WOCE S4 Pacific section. The dots indicate CTD/rosette stations, the dots in circles – with additional biological work. Solid lines with arrows are stream lines of the mean surface geostrophic current (Gordon and Molinelli, 1982). The dashed line is 1000 m isobath. The dashed-dotted line shows the mean position of sea ice edge in March, 1992. ACC and RG indicate the Antarctic Circumpolar Current and the Ross Gyre.

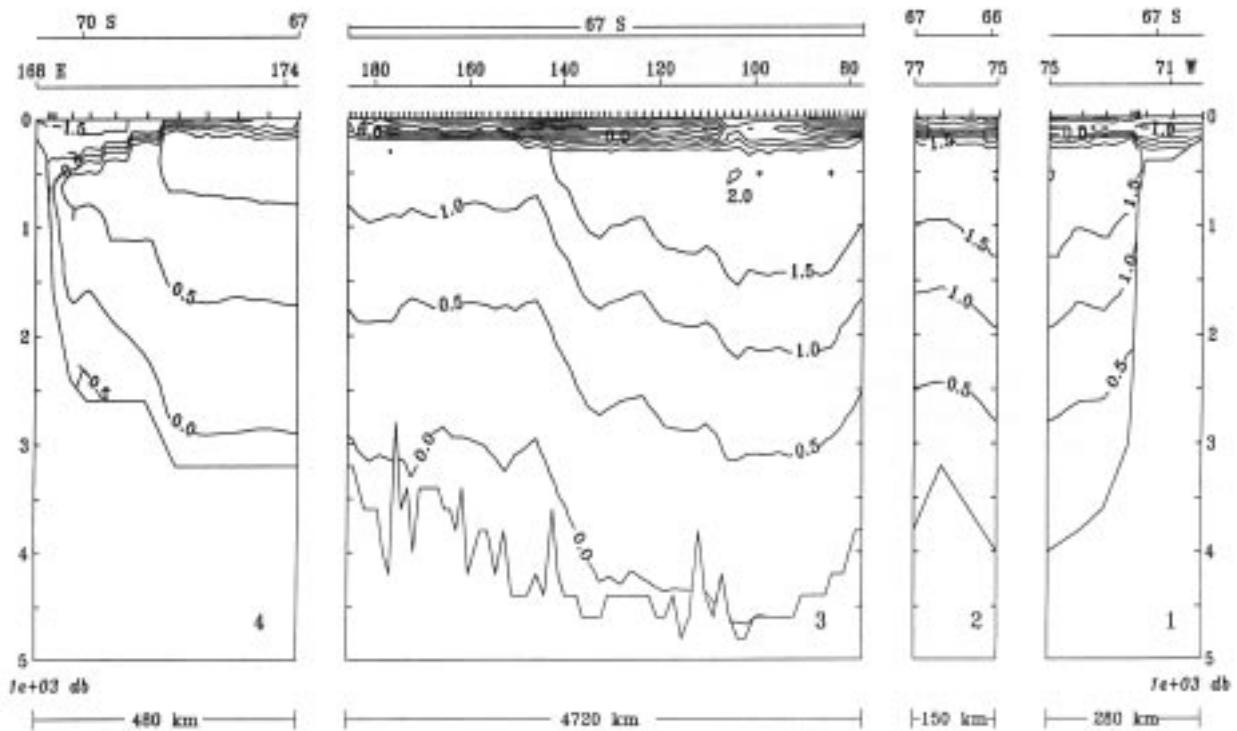


Figure 2. Potential temperature ($^{\circ}\text{C}$) in the S4 section from the Antarctic Peninsula (70°W) to the Pennell Coast (168°E). Positions of the section's parts 1, 2, 3 and 4 can be seen in Figure 1. Horizontal scale for part 3 is five times less than that for parts 1, 2 and 4. The marks on the ocean surface line indicate CTD stations.

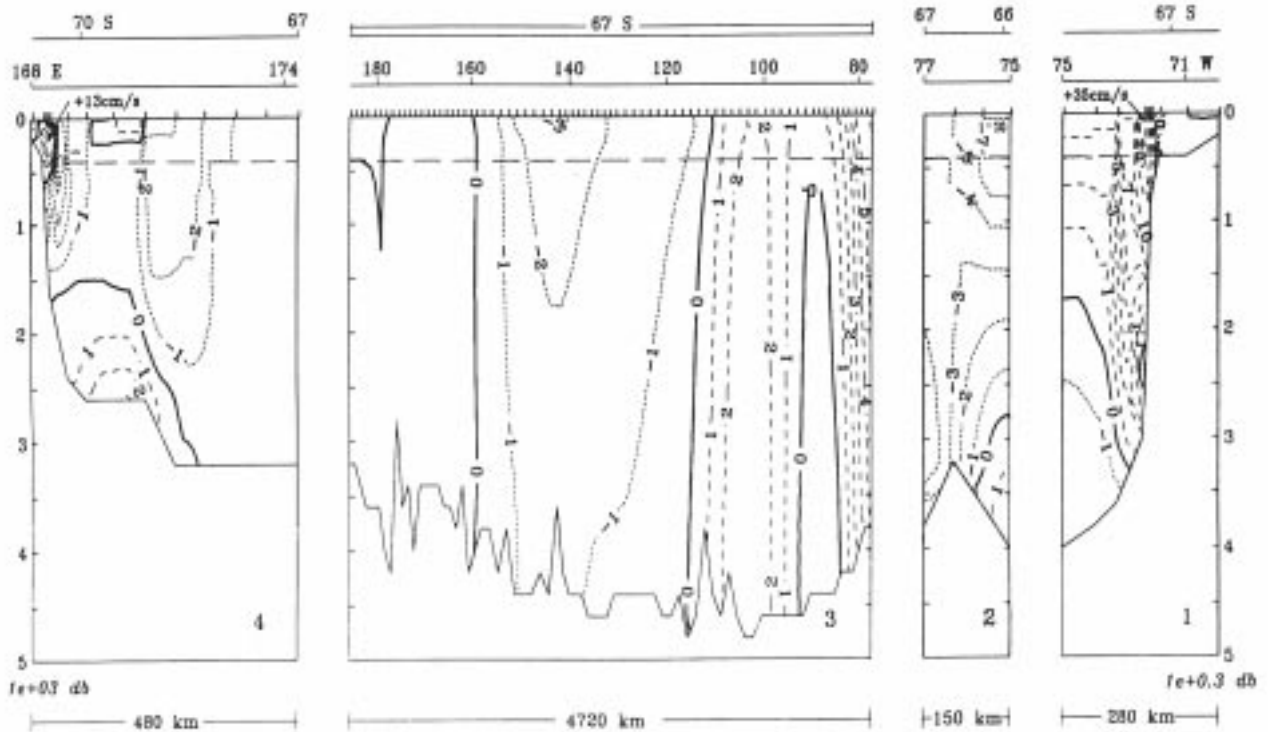


Figure 3. Large-scale geostrophic currents (cm/s) normal to the different parts of Section S4. Horizontal scale for part 3 is five times less than that for parts 1, 2 and 4. The long-dashed isolines and positive values of velocity indicate current out of the Antarctic area (AAA) southward of the S4, short-dashed isolines and negative velocities show current into AAA. The long-dashed horizontal line shows 400 m depth with the ADCP data.

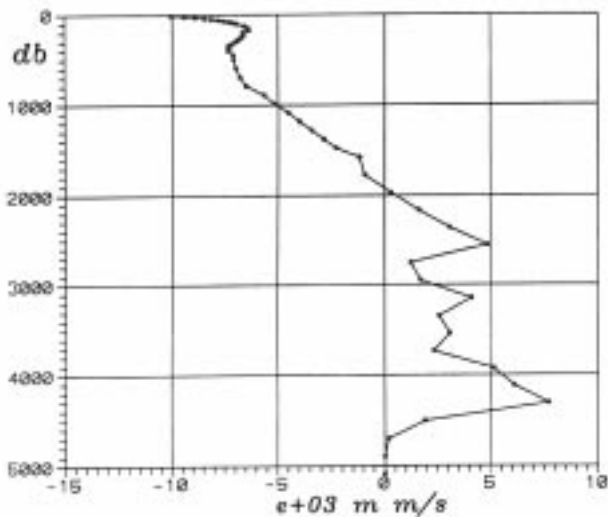


Figure 4. Vertical density (in $10^3 \text{ m}^2 \text{ s}^{-1}$) of the baroclinic volume transport across the entire S4 section. Positive values correspond to the current out of the Antarctic Area.

The curve on Fig. 4 was obtained by integrating the baroclinic component of the geostrophic velocity, normal to the section (Fig. 3), along the whole section at every level. The integral transport in each direction, according to Fig. 4, is 7.9 Sv, which is 4 times less than the total baroclinic transport in each direction (33.0 Sv, Table 1) calculated separately from the opposite transport. The barotropic component of the geostrophic current (Table 1) is determined as the current averaged over the full depth; the baroclinic component is the difference between the total and the barotropic currents. Dividing 7.9 Sv (Fig. 4) by $2.7 \times 10^6 \text{ km}^2$, which is the area between the S4 and the 2000 m isobath at the Antarctic continental slope, we obtain $2.9 \times 10^{-4} \text{ cm/s}$ as the mean downwelling velocity at the 1750 m depth (Fig. 4) in this region.

The values of heat transport across the entire section and separately across its parts with the currents out of and into the AAA (the last column of the second half of Table 1) were computed by the integration of the heat transport density $c_p \rho v \theta$, where, for simplicity, $c_p = 4.2 \times 10^3 \text{ J/kg/}^\circ\text{C}$, $\rho = 1.0 \times 10^3 \text{ kg/m}^3$, v is normal to the section velocity component (positive for the direction out of AAA), θ is the potential temperature, over the corresponding section's areas. Positive value of the integral heat transport (0.077 pW, Table 1) is due to the coupling of the rather strong and predominantly barotropic currents out of AAA and extremely high water temperature at 77–82 and 87–115°W (Figs. 2 and 3). It is known, however, that the large-scale barotropic geostrophic current is rather unstable, being connected with the variations in the large-scale wind field and having typical time scale (period divided by 2π of the order of 5 days (for example, General Circulation of the Southern Ocean, 1986). In this situation the calculated distribution of the barotropic current along S4 could not really be interpreted as a reliable mean distribution during

Table 1. Volume and heat transport across Section S4

	Volume transport [Sv]		
	Barotropic current	Baroclinic current	Total current
Out of the AAA	131.3	33.0	136.7
Into the AAA	-131.3	-33.0	-136.7
Integral transport	0.0	0.0	0.0
	Heat transport [pW] θ in $^\circ\text{C}$		
	By barotropic current	By baroclinic current	By total current
Out of the AAA	0.435	0.066	0.459
Into the AAA	-0.326	-0.098	-0.382
Integral transport	0.109	-0.032	0.077

the section's occupation. On the other hand, the large-scale baroclinic geostrophic current is much more stable with the typical time scale at least an order as great as that for the barotropic current. The second column of the second half of Table 1 presents baroclinic heat transport totally for the S4 and separately in two opposite directions, and Fig. 5 shows the result of integration of the baroclinic heat transport density along the whole section at every level. The integral over the depth of the distribution shown in Fig. 5 is equal to -0.032 pW , as it can be seen in Table 1. The negative values of heat transport density below 1800 m depth (Fig. 5) can be explained, first, by the negative water temperature at the bottom in the middle and the western parts of the S4 (Fig. 2), and, second, by the coupling of the relative high temperature and the rather high baroclinic current into the AAA at the depths below 1800 m at 77–96°W (Figs. 2 and 3). At the same time we should emphasise, that the integral heat transport across any ocean section, for which the

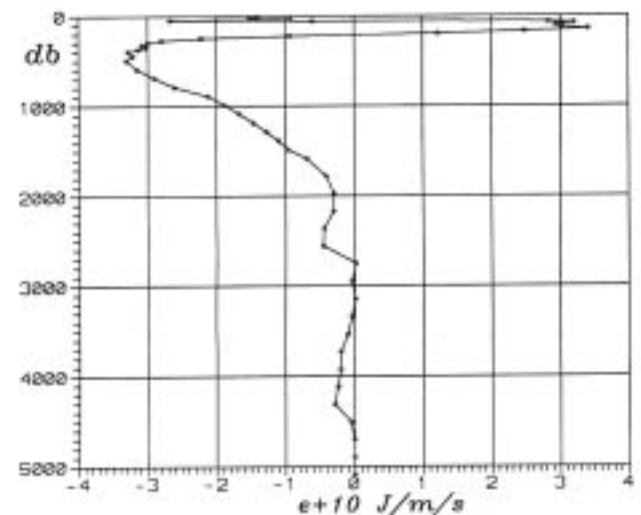


Figure 5. Vertical density (in 10 J/m/s) of the heat transport across the entire S4 section, induced by the baroclinic component of the geostrophic current. Negative values correspond to heat transport (referred to temperature in $^\circ\text{C}$) into the Antarctic area.

corresponding integral volume transport is zero (as we have for the integral baroclinic volume transports) does not depend on the temperature scale used. This circumstance gives an unquestionable physical sense to the calculated 0.032 pW integral baroclinic heat transport across the S4 towards the Antarctic Continent. As could be seen from Figs. 2, 3 and 5, the combination of the rather high theta and the relatively strong baroclinic currents into the AAA at 200–2000 m depths within a very wide region at 95–160°W (see the slope of the isolines at 95–115°W in Fig. 3) gives the main contribution to this integral heat transport. The 0.032 pW corresponds to 1×10^{21} J per year which is one order lower than the annual heat flux from the ocean to the atmosphere in the entire Antarctic area southward of the South Polar Front (Gordon, 1988). Because the area between the S4 and the Antarctic Slope is about one order less than the area between the South Polar Front and this Slope (2.7×10^6 and $35 \times 10^6 \text{ km}^2$ 10^{21} J per year) can be considered as a very possible mechanism of compensation of the ocean/atmosphere heat exchange, at least, in the Pacific Sector of the Antarctic. It is reasonable to suppose that this heat transport is a sign of the overturning process near the Antarctic Continent connected with the water cooling in the upper ocean layer near the Antarctic Continent. Difference between our results and the results of Saunders and Thompson (1993) who obtained zero thermohaline (baroclinic) transport across the 60°S circle can be connected, in particular, with the difference in latitudes and

with the fact that we considered only the Pacific sector of the Southern Ocean.

Acknowledgements

The CTD measurements in the S4 section were made with the USA equipment provided for the Akademik Ioffe cruise by the USA scientific team, headed by Dr Jim Richman and Dr Jim Swift. All these measurements and data acquisition were carried out jointly by the Russian and the USA scientists and technicians. This work was supported by grant No. 94-05-16179-a of the Russian Foundation for Fundamental Researches and by grant No. NDX000 of the International Science Foundation.

References

- General Circulation of the Southern Ocean, 1986: A Report by SCOR Working Group 74, October 1985. WCP-108, WHO/TD-N 86.
- Gordon, A.L., 1988: Spatial and temporal variability within the Southern Ocean. In: Antarctic Ocean and Resources Variability (ed: D. Sahrhage), Springer-Verlag, Berlin, 41-56.
- Gordon, A.L., and E.J. Molinelli, 1982: Southern Ocean Atlas. Columbia University Press, N.Y.
- Saunders, P.M., and S.R. Thompson, 1993: Transport, heat and freshwater fluxes with a diagnostic numerical model (FRAM). *J. Phys. Oceanogr.*, 23(3): 452-464.

The Weddell Gyre Study 1989 – 1993

Eberhard Fahrbach, Gerd Rohardt, Michael Schröder and Volker Strass, Alfred-Wegener-Institut für Polar- und Meeresforschung, Postfach 120161, 27515 Bremerhaven, Germany

A cyclonic gyre controls the advection of source waters into the formation areas of bottom water in the southern and western parts of the Weddell Sea and the subsequent transport of modified water masses to the north. Determination of the structure of the Weddell Gyre and of the associated transports was one of the objectives of the "Weddell Gyre Study" which began in September 1989 and ended in January 1993. The collected data set comprises records of moored current meters and profiles of temperature and salinity distributed along a transect between the northern tip of the Antarctic Peninsula and Kapp Norvegia. The current meter data are kept under WOCE code SCM7 and the hydrographic measurements under WOCE repeat hydrography line SR4.

The field work began with the deployment of eight current meters on three moorings during the "European Polarstern Study" in February 1989 which were recovered in February 1990. During the first survey of the "Weddell Gyre Study", carried out in September and October 1989 and named the "Winter Weddell Gyre Study", 24 current

meters on 7 moorings were deployed from RV Polarstern along a 2100-km long line between Joinville Island, near the northern tip of the Antarctic Peninsula and Kapp Norvegia (Augstein *et al.*, 1991). These moorings were recovered in November and December 1990, during the "Summer Weddell Gyre Study", and a new set of 21 moorings with 64 current meters was laid (Fig. 1, Fahrbach *et al.*, 1992). Of these, 18 moorings with 49 current meters were recovered in December 1992 and January 1993 (Fahrbach *et al.*, 1994a). Due to unexpected high power consumption by the current meters, most instruments did not record during the entire two-year period of the second deployment, but for only one year. Five of the recovered instruments had failed completely.

The full set of current meter data collected during the three years (Fig. 2) came from 60 instruments, 53 of which were Aanderaa models RCM4/RCM5 or RCM7/RCM8. The remaining 7 instruments were acoustic devices, EG&G model ACM-2. These current meters were installed during the second deployment period, but only at the greatest

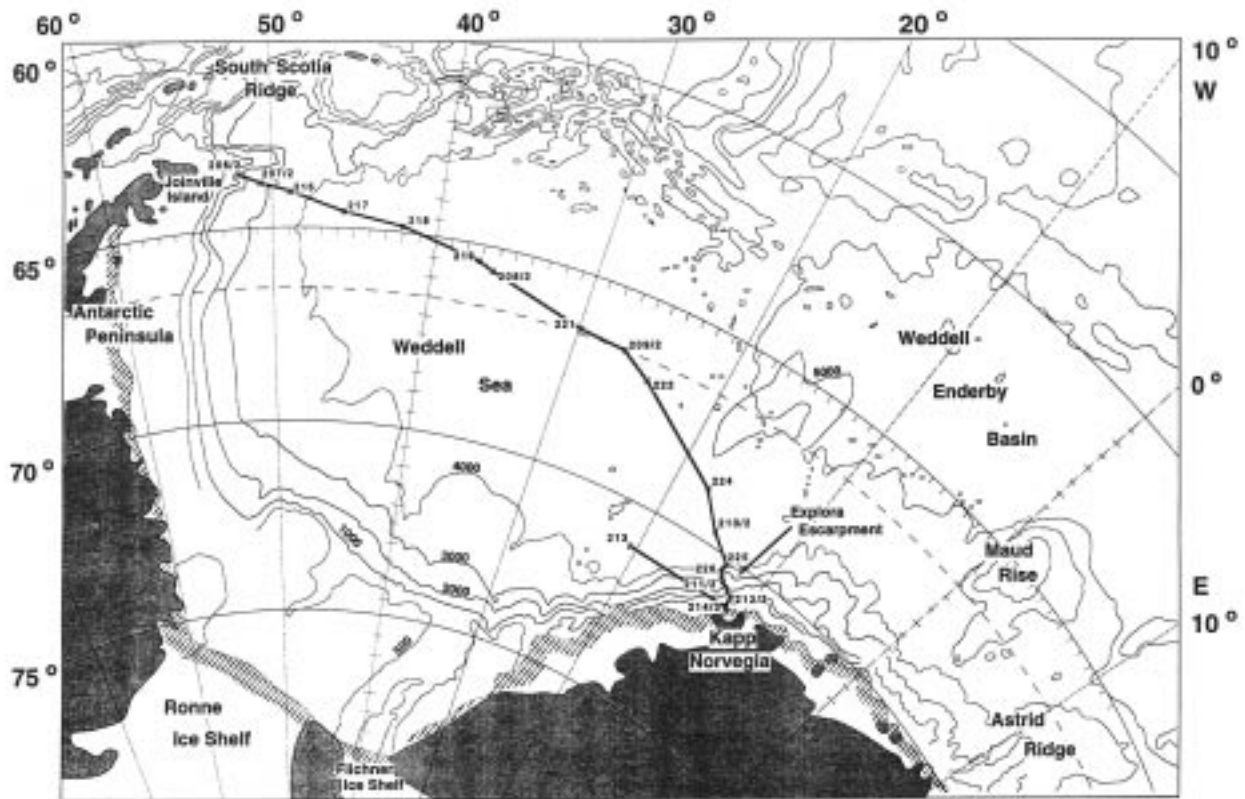


Figure 1. Location of the transect from Kapp Norvegia to Joinville Island at the northern tip of the Antarctic Peninsula with moored current meter and CTD measurements made during the Weddell Gyre Study 1989-1993. The numbers indicate the mooring code. The depth contours are provided by H. Hinze on the basis of GEBCO 5.18 and soundings carried out during the drift of Ice Station Weddell (Gordon et al., 1993) and Polarstern-cruise X/7 (Fahrbach et al., 1994a).

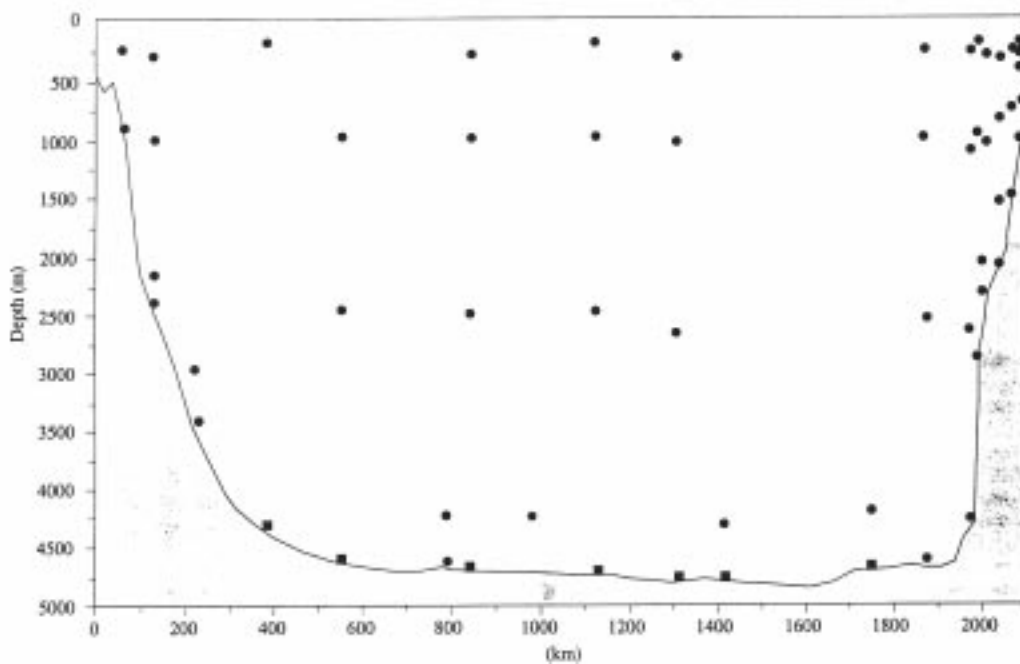


Figure 2. Location of the current meters on the transect between Joinville Island (left) and Kapp Norvegia (right) deployed during the periods February 1989 to February 1990, September 1989 to December 1990 and December 1990 to January 1993.

depths (50 m above the sea floor, to be above the bottom boundary layer). The uppermost current meters were placed in the depth range of 200–300 m, in order to stay clear of passing icebergs. Methods used for data processing and further information on the performance of the instruments are documented by Rohardt et al. (1992; in press).

Complementing the direct current measurements, full-depth profiles of temperature and conductivity were obtained with rosette-mounted NBIS Mark IIIb CTDs. Water samples were obtained at 24 levels on each cast and analyzed

for salinity with a Guildline Autosol 8400A. These were used for calibrating conductivity of the CTDs, which were calibrated for temperature and pressure before and after each cruise at Scripps Institution of Oceanography. The laboratory calibrations were further checked at sea with additional pressure sensors, digital thermometers, and protected and unprotected mercury thermometers. After all checks for data quality, the CTD data obtained below the thermocline has been determined to be better than 0.003 in salinity, 3 mK in temperature, and 3 db in pressure.

The circulation pattern on the transect is dominated by stable boundary currents of several hundred kilometre width at the eastern and western sides of the basin (Fig. 3). They are of comparable size on both sides and provide nearly 90% of the volume transport of the gyre which amounts to 29.5 Sv ($1 \text{ Sv} = 10^6 \text{ m}^3 \text{ s}^{-1}$, *Fahrbach et al.* 1994b). In the interior a weak anticyclonic cell of 800 km diameter transports less than 4 Sv. Apart from the continental slopes, the near-bottom currents are in opposite direction to those in the water column above, indicating a significant baroclinic component of the current field. The intensity of the boundary currents is subject to seasonal fluctuations, whereas in the interior time scales from days to weeks dominate. The large scale circulation pattern is persistent during the years 1989 to 1991.

On the basis of the current pattern and the obtained temperature and salinity profiles (Fig. 4) heat and salt transports into the area south of the transect and out of it were calculated. The heat transport into the southern

Weddell Sea is estimated to $3.5 \times 10^{13} \text{ W}$. This implies an equivalent heat loss through the sea surface of 19 W m^{-2} , as an average value for the area south of the transect. The derived salt transport is not significantly different from zero; consequently, the salt gain by sea ice formation has to compensate almost entirely the fresh water gain from the melting ice shelves and from precipitation. Estimation of water mass formation rates from the thermohaline differences of the inflow and outflow through the transect indicates that 6.0 Sv of Warm Deep Water are transformed into 2.6 Sv of Weddell Sea Bottom Water, into 1.2 Sv of Weddell Sea Deep Water, and into 2.2 Sv of Surface Water.

Deep and bottom water formation in the Weddell Sea is the major source of the bottom water of the world ocean. Measurements made in the northwestern Weddell Sea between 1989 and 1993 during the 'Weddell Gyre Study' indicate that the outflow of young bottom water in the western boundary current of the Weddell Gyre is dominated by a rather fresh water mass (Fig. 4) which obtains its thermohaline characteristics by mixing of deep water with a flow from the shelf in front of the Larsen Ice Shelf. The more saline source water mass, which is necessary to maintain the thermohaline properties of the Weddell Sea Deep Water, is less prominent in the bottom water outflow. The transport of bottom water with the western boundary current of the Weddell Gyre ranges from 1 to $4 \times 10^6 \text{ m}^3 \text{ s}^{-1}$. The outflow is subject to a seasonal cycle with minimum temperatures and maximum velocities in early austral winter (Fig. 5, *Fahrbach et al.*, submitted).

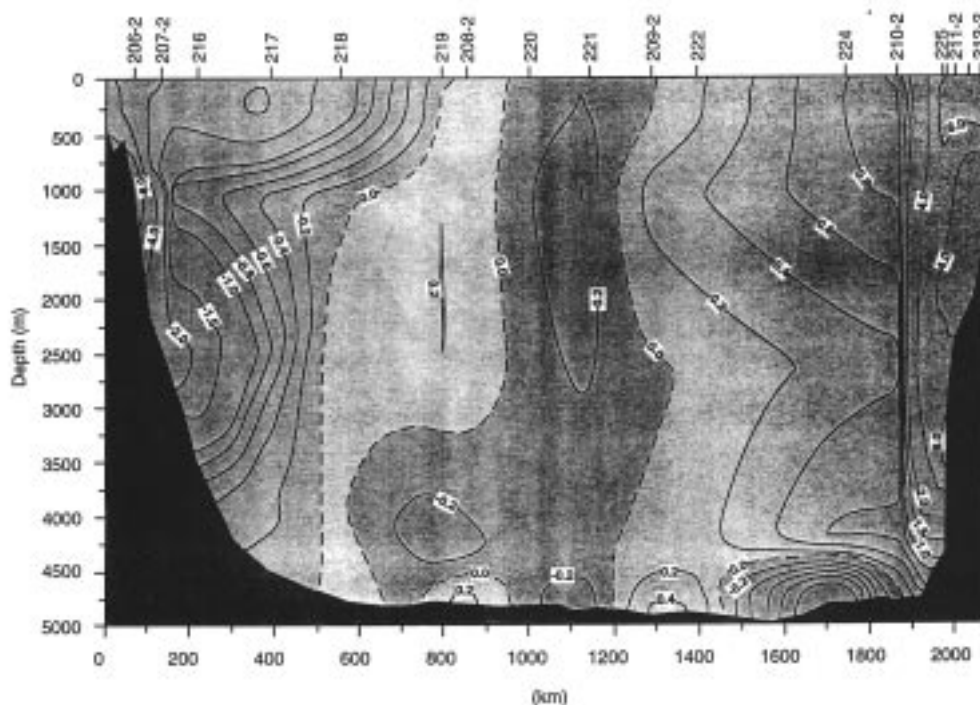


Figure 3. Distribution of the mean current component (cm s^{-1}) normal to the cross section through the Weddell Gyre between Joinville Island (left) and Kapp Norvegia (right), revealed by the composite data set from February 1989 to January 1993; negative velocities and dark shading means outflow to the northeast, positive means inflow to the southwest. For the locations of the current meters see Figure 2.

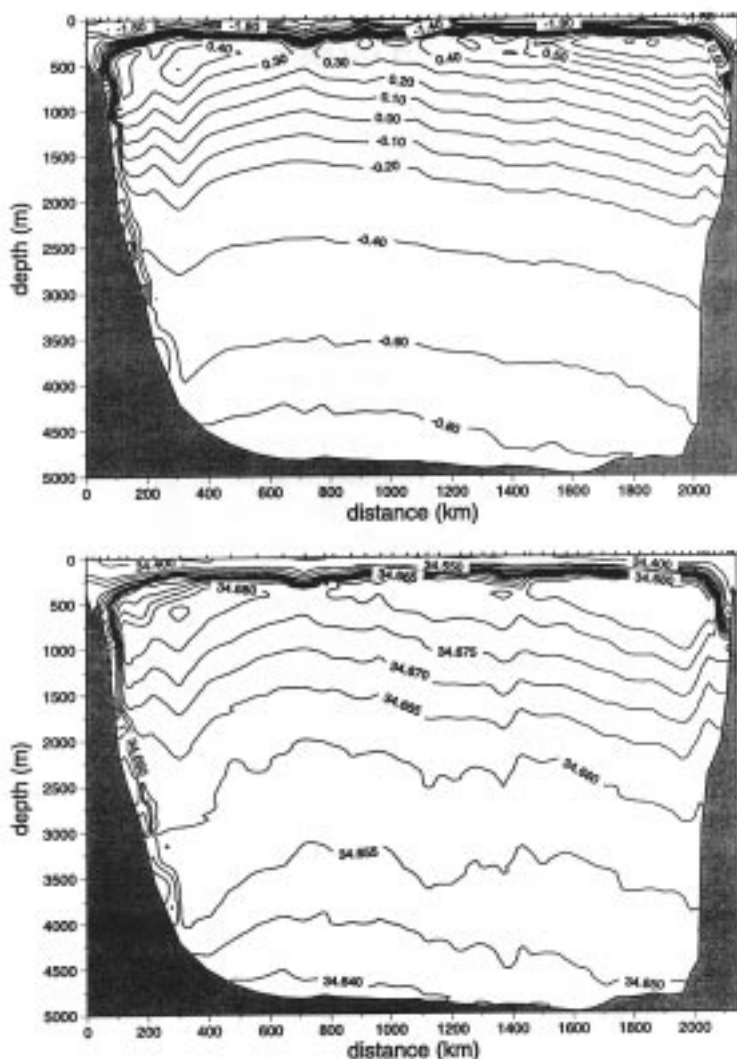
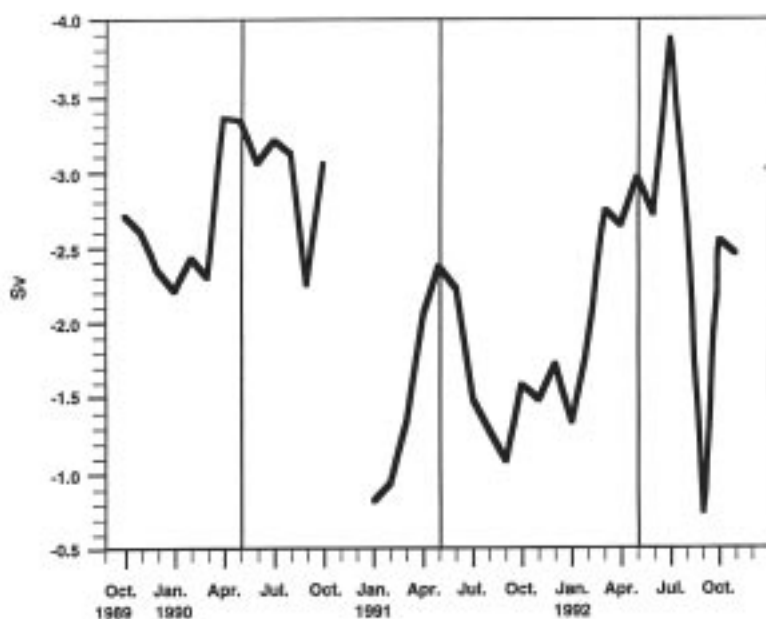


Figure 4. Potential temperature in °C (top) and salinity (bottom) on the cross section through the Weddell Gyre between Joinville Island (left) and Kapp Norvegia (right), measured in November and December 1990.



References

- Augstein, E., N. Bagriantsev and H.W. Schenke (eds.), 1991: The Expedition ANTARKTIS VIII/1-2, 1989, with the Winter Weddell Gyre Study of the Research Vessels "Polarstern" and "Akademik Fedorov". Ber. Polarforsch., 84, 134pp.
- Fahrbach, E., with contributions of the participants, 1992: Cruise Report ANT IX/2, in Bathmann, U., M. Schulz-Baldes, E. Fahrbach, V. Smetacek and H.-W. Hubberten (Eds.). The Expeditions ANTARKTIS IX/1-4 of the Research Vessel "Polarstern" in 1990/91. Ber. Polarforsch. 100, 403pp.
- Fahrbach, E., with contributions of the participants, 1994a: Cruise Report ANT X/7, in Bathmann, U., E. Fahrbach, G. Krause and V. Smetacek (Eds.). The Expeditions ANTARKTIS X/6-8 of the Research Vessel "Polarstern" in 1992/93. Ber. Polarforsch., 135, 127-197.
- Fahrbach, E., G. Rohardt, M. Schröder, and V. Strass, 1994b: Transport and structure of the Weddell Gyre. Ann. Geophysicae, 12, 840-855.
- Fahrbach, E., G. Rohardt, N. Scheele, M. Schröder, V. Strass, and A. Wisotzki: Formation and discharge of Deep and Bottom Water in the Northwestern Weddell Sea. Submitted to J. Mar. Res.
- Gordon, A.L., and Ice Station Weddell Group of Principal Investigators and Chief Scientists, 1993: Weddell Sea Exploration from Ice Station, Eos Trans. AGU, 74, 121 and 124-126.
- Rohardt, G., E. Fahrbach, G. Krause, and V.H. Strass, 1992: Moored current meter and water level recorder measurements in the Weddell Sea 1986-1990, Berichte aus dem Fachbereich Physik, Alfred-Wegener-Institut für Polar- und Meeresforschung, 28, Bremerhaven, Germany.
- Rohardt, G., E. Fahrbach, and V.H. Strass: Moored current meter measurements in the Weddell Sea 1991-1993, Berichte aus dem Fachbereich Physik, Alfred-Wegener-Institut für Polar- und Meeresforschung, Bremerhaven, Germany, in press.

Figure 5. Time series of monthly average transport of Weddell Sea Bottom Water across the transect off Joinville Island in Sv ($1 \text{ Sv} = 10^6 \text{ m}^3 \text{ s}^{-1}$), obtained from moorings 206, 207, and 216 from October 1989 to November 1992.

Bottom Water Anomaly at the Subantarctic Front on Greenwich Meridian

M. Schröder, M. Hoppema and A. Wisotzki, Alfred-Wegener-Institut für Polar- und Meeresforschung, Postfach 120161, D-27515 Bremerhaven, Germany

As part of the World Ocean Circulation Experiment (WOCE) the oceanographic programme during the winter cruise (ANT X/4) of RV Polarstern in 1992 focused on two hydrographic sections: A12 which serves simultaneously as one repeat of section SR2, between South Africa and the Antarctic continent, and SR4 in the Weddell Sea, connecting Kapp Norvegia and the tip of the Antarctic Peninsula. For locations see the report of Hoppema *et al.* in this volume. For both sections the measurements represent the first mid-winter oceanographic observations in that area. The oceanographic programme comprised 115 CTD-stations in total. 101 deep casts with vertical temperature and conductivity profiles and 24 water samples at each station for salinity, oxygen, silicate, phosphate, nitrate, nitrite were measured for physical oceanography purposes and 14 special shallow casts for biological use. Tracer samples were collected for Tritium, Helium, F-11, F-12 and oxygen isotopes O-16/O-18. The section A12/SR2 along the Greenwich Meridian consisted of 71 deep profiles, the section SR4 across the Weddell Sea of 28 profiles. For calibration purposes two additional deep casts were taken.

The observation in winter of the large scale hydrographic conditions and in particular the structure of the oceanic fronts of the Southern Ocean (the Subtropical Front (STF), the Subantarctic Front (SAF), the Polar Front (PF), and the Continental Water Boundary (CWB)), was one of the objectives of the cruise. In general the hydrographic transects revealed the large scale features described by Whitworth and Nowlin (1987). The horizontal differences in temperature and salinity across the fronts were measured in the near surface layer with a thermosalinograph as:

	ΔT (°C)	ΔS
STF:	7.0	1.0
SAF:	3.5	0.4
PF:	1.5	0.2

Except for the Polar Front the observed gradients were higher than in the summer season (Bathmann *et al.*, 1992). In ice covered regions the instrument did not record, because of freezing within the pump system. Therefore, values for the gradients at the CWB could not be determined. The location of the oceanographic fronts and the main water mass characteristics in the Atlantic sector of the Southern Ocean along the Greenwich Meridian are shown in Fig. 1. Looking from north to south between STF and SAF, the upper water column (0–1000 m) is dominated by the surface waters of the subtropical gyre (north of the STF) and Subantarctic Surface Water (SASW) which are high in salinity and temperature but poor in oxygen and nutrients. Between the Subantarctic and the Polar Front the Antarctic Intermediate Water (AAIW) which is characterised by low salinity and high oxygen values spreads towards the north.

In the upper 200 m south of the PF the water is cold, fresh, rich in oxygen and high in nutrients as compared to the SASW. It is composed of Antarctic Surface Water (AASW) and/or Winter

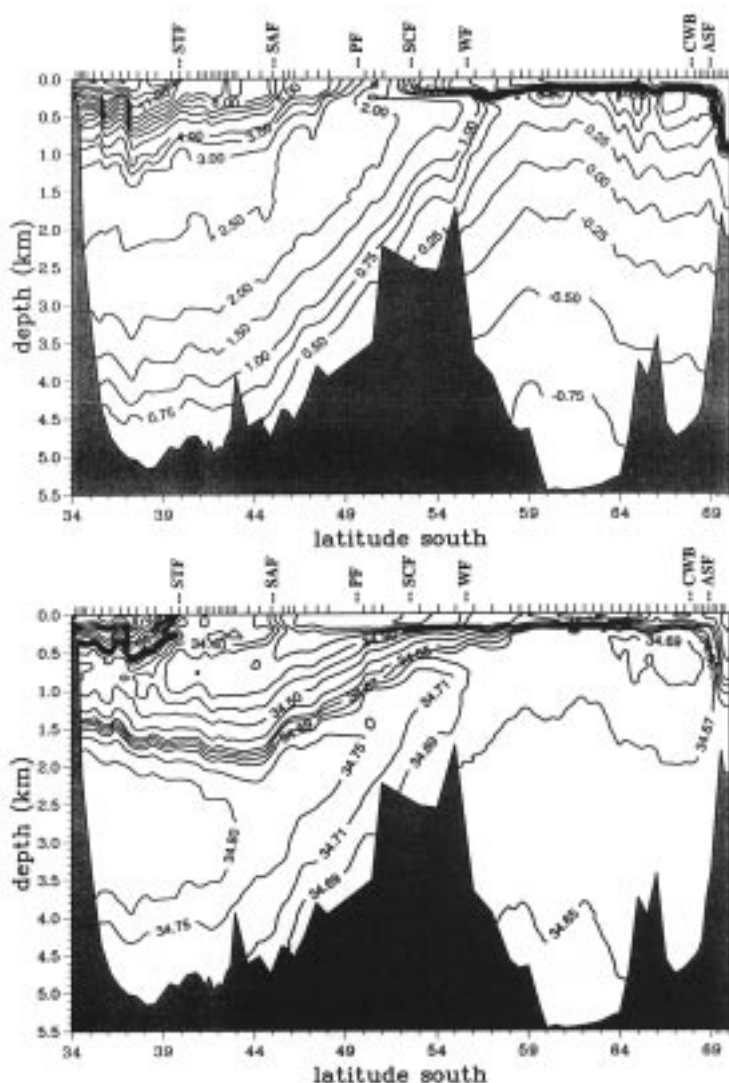


Figure 1. Vertical sections of potential temperature and salinity observed by RV Polarstern in June 1992 between South Africa and the Antarctic Continent. STF = Subtropical Front, SAF = Subantarctic Front, PF = Polar Front, SCF = Southern Front of the Circumpolar Current, WF = Weddell Front, CWB = Coastal Water Boundary, ASF = Antarctic Slope

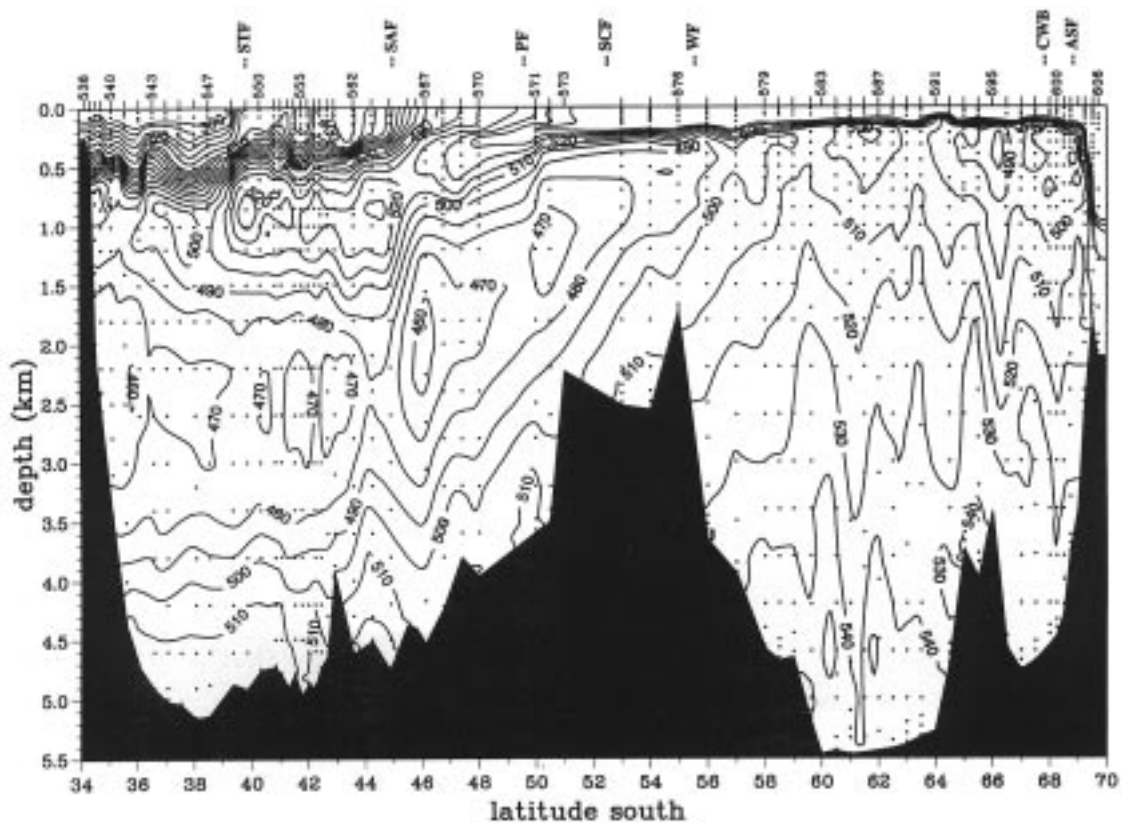


Figure 2. Vertical section of NO in $\mu\text{mol/kg}$ observed by RV Polarstern in June 1992 between South Africa and Antarctic Continent.

Water (WW) which is cooled down to the freezing point. Near the continent, the pycnocline isolating the convective layer from the Warm Deep Water (WDW) underneath deepens towards the shelf down to 600 m. At the shelf break less saline waters of the Coastal Current (CC) regime appear which have lower oxygen but higher nutrient concentrations as the surrounding water masses.

The deep ocean (>1000 m) is dominated by the Circumpolar Deep Water (CDW) with a thickness of more than 3000 m. Upper CDW (UCDW) with its source in the Indian and Pacific oceans with high nutrient and low oxygen values can be distinguished from Lower CDW (LCDW) originating from the North Atlantic Deep Water (NADW) marked by a maximum in salinity and oxygen and a minimum in nutrients. Below, Antarctic Bottom Water (AABW) spreads to the north as a tongue of cold, fresh water with high oxygen and nutrient values. It fills the lowest 500 m above the bottom north of the mid-ocean ridge at 56°S.

Near the Subantarctic Front anomalously high concentrations of nitrate and phosphate were observed while temperature and salinity did not show unusual patterns. The features are most obvious in 'NO', a quasi-conservative tracer defined as $\text{'NO'} = [\text{O}_2] + 9[\text{NO}_3^-]$ by Broecker (1974) under the assumption that for each molecule of oxygen which is consumed by biological degradation nine molecules of nitrate are liberated. Oxygen and nutrients are separately integrated in production and decomposition of organic

matter and represent less powerful tracers for water masses as the combination of both concentrations namely 'NO'.

North of the Subantarctic Front at depths between 1500 and 3500 m NO is significantly increased compared to adjacent stations. Additionally a maximum of 520 $\mu\text{mol/kg}$ is found near the bottom. The anomaly cuts the southward penetrating tongue of North Atlantic Deep Water obvious as a minimum in NO in two separate regimes (Fig. 2).

Data from a summer cruise of RV Meteor in 1990 (ME 11/5) in Drake Passage and south of South Africa were used to identify the origin of that structure. In Drake Passage high concentrations of nutrients and NO were also measured near the Subantarctic Front, however, no maximum was found at the bottom. Near the Greenwich meridian the Meteor data did not reveal such anomalies indicating on the intermittency of that feature.

Mixing diagrams of all parameters measured in winter 1992 suggest that the part of the nutrient anomaly in mid depth between 1500 and 3500 m had its origin in the Pacific. It was observed at the Drake Passage in 1990 and approximately two and a half years later at the Greenwich Meridian. The near bottom maximum can not be found in Drake Passage and the only water mass which has consistent properties as a source water is Weddell Sea Deep Water between 500 and 2500 m (Fig. 3). This points to the Weddell Sea as the origin, but intermittency of the occurrence in Drake Passage still retains some uncertainty in our conclusion.

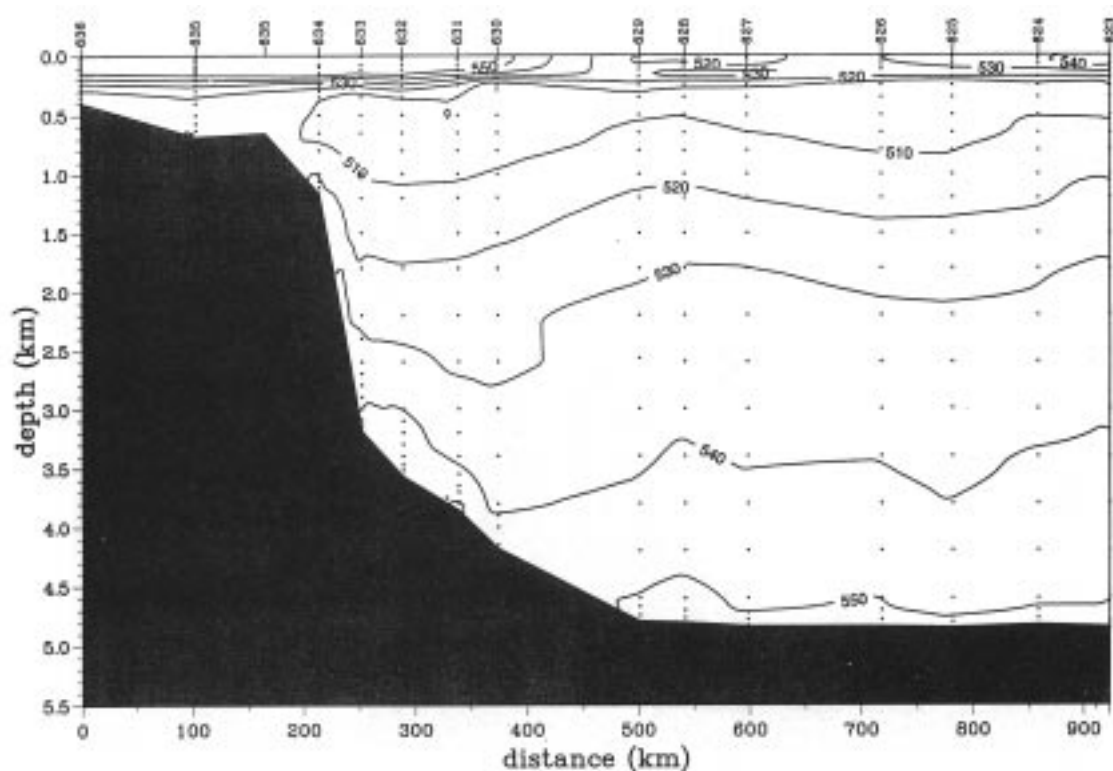


Figure 3. Vertical section of NO in $\mu\text{mol/kg}$ observed by RV Polarstern in July 1992 in the inner Weddell Sea.

Assuming the Weddell Sea as the more probable source, the route from the Weddell basin to the Subantarctic Front at 45°S , 0°E has still to be identified. The outflow of Weddell Sea Deep Water through gaps in the South Scotia Ridge and its dilution within the Scotia Sea is likely to be involved. A possible continuation of the flow runs east of the South Sandwich Arc and must be focused into distinct streaks during its passage through deep gaps in the Mid-Atlantic Ridge, such as the one near 43°S . This leads to the well defined bulge near the bottom underneath the Subantarctic Front. Our observation suggests that upper Weddell Sea Deep Water possibly plays a more important role in the modification of AABW than previously thought.

References

- Broecker, W.S., 1974: Chemical Oceanography. Harcourt Brace Jovanovich, New York, 214pp.
- Bathmann, U., M. Schulz-Baldes, E. Fahrbach, V. Smetacek, and H.-W. Hubberten (eds.), 1992: The Expedition ANTARKTIS IX/1-4 of the Research Vessel "Polarstern" in 1990/91. Ber. Polarforsch., 100: 1-403.
- Whitworth, T., III, and W.D. Nowlin, Jr., 1987: Water masses and currents of the Southern Ocean at the Greenwich Meridian. J. Geophys. Res., 92, 6462-6476.

Carbon Dioxide Investigations During the Weddell Gyre Study

Mario Hoppema and Eberhard Fahrbach, Alfred-Wegener-Institut für Polar- und Meeresforschung, Postfach 120161, 27515 Bremerhaven, Germany

Since 1989 the circulation of the Weddell Gyre has been the subject of an intensive investigation at the Alfred-Wegener-Institut under the title 'Weddell Gyre Study' as part of the German WOCE programme. Emphasis in this study has been on transport measurements of the gyre through mooring arrays with current meters, and on the hydrography through repeated CTD (Conductivity-

Temperature-Depth) sections (*e.g.* see Fahrbach *et al.*, 1994). As of 1992 the Weddell Gyre Study was extended to encompass the investigation on the role of the Weddell Sea and adjacent regions as to the inorganic carbon cycle. Since carbon research has joined the project, TCO_2 measurements were done on two cruises in the Weddell Sea with FS Polarstern (Fig. 1) - TCO_2 means total dissolved

carbon dioxide, *i.e.* the sum of dissolved CO₂, carbonic acid, bicarbonate and carbonate, between which a chemical equilibrium exists. The first cruise was carried out in austral winter between 21 May and 5 August 1992 and included the one time hydrographic WOCE section A12, which is simultaneously a repeat of section SR2 between Cape Town and the Antarctic continent. Due to adverse ice conditions the planned WOCE repeat section SR4, closing off the Weddell embayment between Kapp Norvegia and the tip of the Antarctic Peninsula, could not be completely occupied. The cruise track was shifted in the direction of the South Orkney Islands. Still, unique and valuable data of the wintertime Weddell Sea were collected. During the second cruise in the following austral summer (December 1992/January 1993) section SR4 was nevertheless wholly covered with a very close station spacing.

A main purpose of the CO₂ investigations in the Weddell Sea is to track down whether the region is a source or sink of atmospheric CO₂. We try to tackle this problem by making budget calculations with the support of hydrographic data that are collected simultaneously. Another purpose is to investigate the use of TCO₂ as a water mass tracer in this area. Both of these main purposes will be illustrated below.

In Fig. 2 the vertical section of TCO₂ along the prime meridian from just south of the Subtropical Front to the Antarctic coastline is shown. The TCO₂ distribution combines features seen in the temperature and salinity distributions and thus principally reflects the different water masses in the Antarctic Circumpolar Current (ACC) and the Weddell Sea (compare the classical work of Whitworth and Nowlin (1987) for this region). Also the major frontal systems find an expression in the TCO₂ distribution, both at

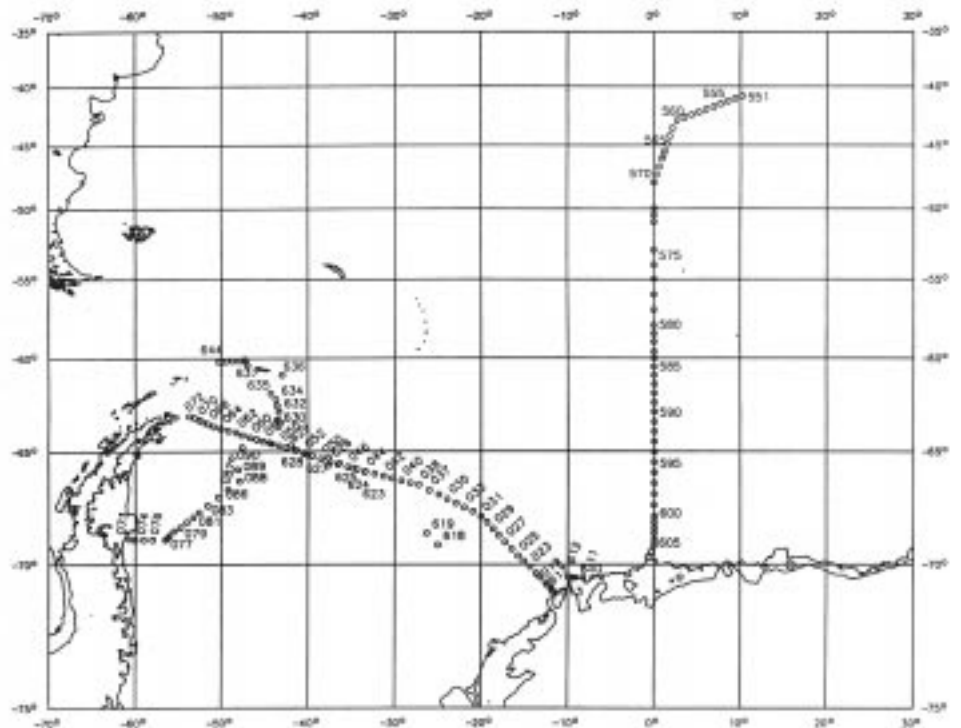


Figure 1. Map of the Atlantic sector of the Southern Ocean showing locations of the summer and winter TCO₂ transects.

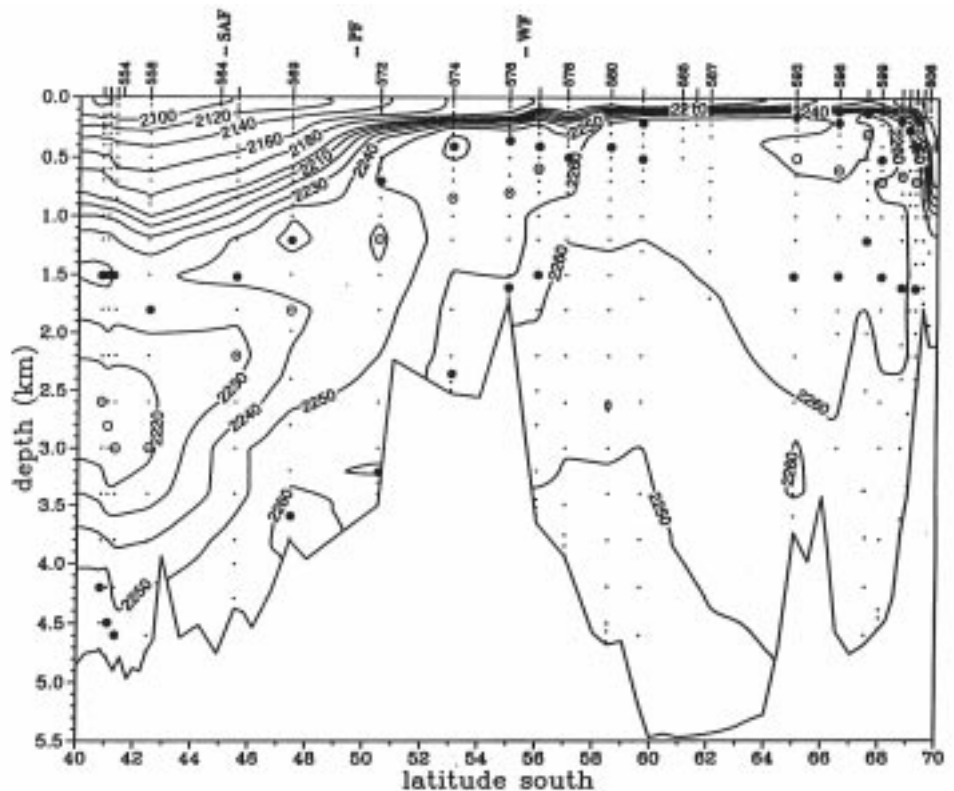


Figure 2. TCO₂ ($\mu\text{mol/kg}$) distribution on the section along the prime meridian from just south of the Subtropical Front (left) to Antarctica (right). Closed circles denote a TCO₂ maximum, open circles a TCO₂ minimum. SAF, Subantarctic Front; PF, Polar Front;

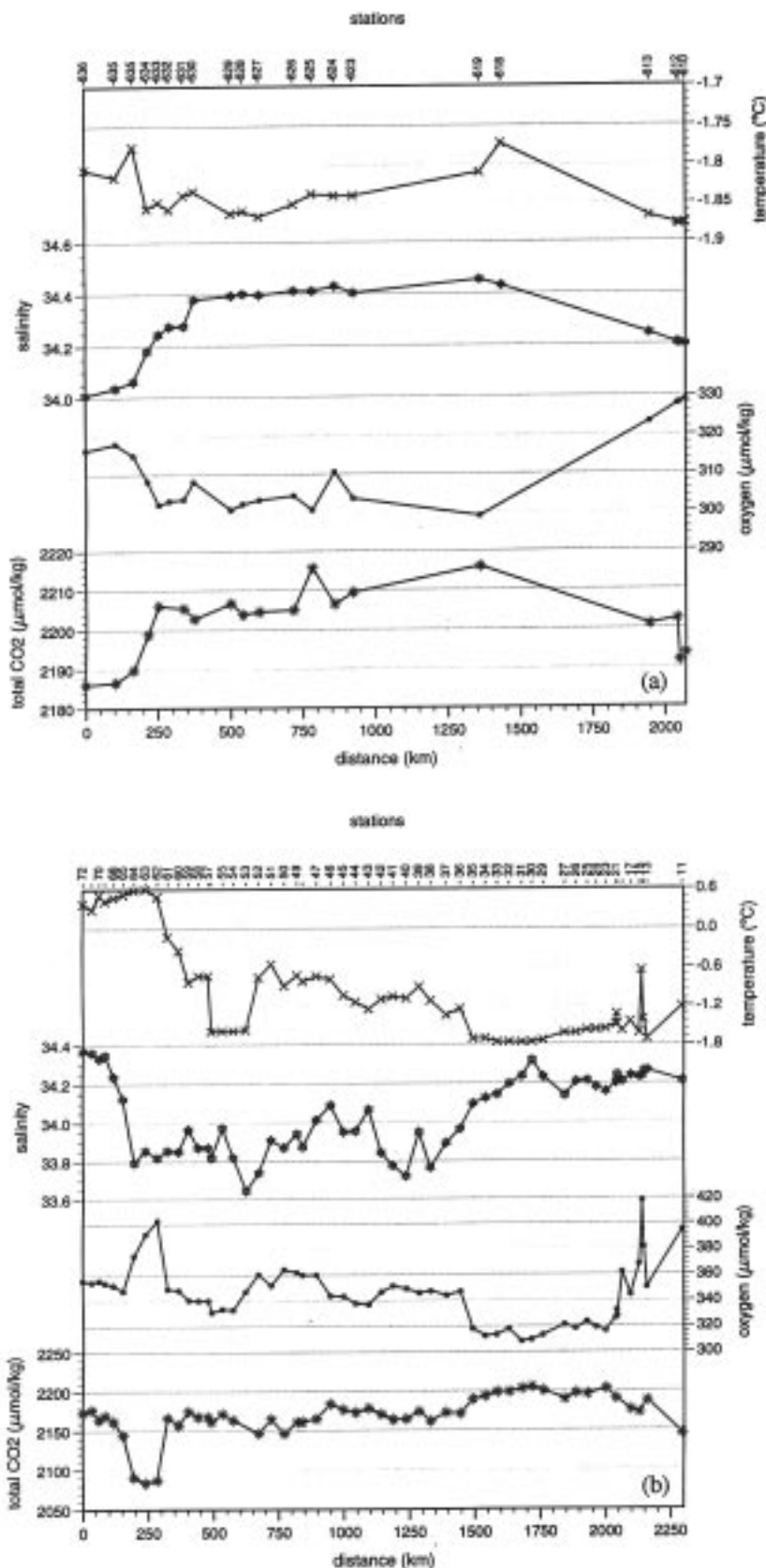


Figure 3. Surface transects of the winter and summer cruises in the western Weddell Sea. (a) Winter transect between Kapp Norvegia (right) and the South Orkney Islands (left); (b) summer transect between Kapp Norvegia (right) and the tip of the Antarctic Peninsula (left).

the surface and in deeper portions of the water column. However, it adds new features as well. North of the Subantarctic Front the low-TCO₂ tongue of North Atlantic Deep Water is recognized around 2500–3000 m depth. As the tongue penetrates the ACC it induces a TCO₂ maximum at about 1500 m. Both this maximum and minimum of the Circumpolar Deep Water (CDW), which is the water mass that occupies most of the ACC water column, rise southwards. Only lower CDW is able to enter the Weddell Sea. CDW that recently entered the Weddell Gyre is detected in the southernmost part of the section (65–70°S). Upon entering the Weddell Sea the TCO₂ minimum of the lower CDW is maintained (at about 500 m). Due to its specific properties with respect to TCO₂ the vertical extent of the newly injected CDW layer can also be detected. A shallow TCO₂ maximum is induced by the overlying low-TCO₂ surface water and indicates the upper boundary of that layer. The lower boundary is revealed by a maximum at about 1500 m (Fig. 2). Our data show that this deep TCO₂ maximum stays essentially intact in the Weddell Sea, in contrast with the upper part of the CDW stratum, which is thoroughly modified through vertical transport and shelf/slope processes. TCO₂ turns out to be a good tracer for the recent CDW on its course through the Weddell Sea.

In the ACC-part of the section (*i.e.* north of the Weddell Front, WF) a faint TCO₂ maximum is observed some 200–300 m above the bottom. We interpret this as being the upper boundary of the Antarctic Bottom Water, that mainly originates in the Weddell Sea. The occurrence of a TCO₂ maximum follows from injection of low-TCO₂ deep and bottom water from the Weddell Sea into the bottom layer of the ACC. The properties of this AABW bottom layer (TCO₂, potential temperature, salinity and oxygen) correspond to those from a depth of around 1000 m in the Weddell Sea. Mixing on its way between the Weddell Sea and the ACC will, however, modify the properties of the nascent bottom layer, which implies that the water possibly originates from another depth than the one where the properties are found to be identical.

First steps were set on the path of our other main intention, *i.e.* budget calculations. In Fig. 3 the surface transects through the western Weddell Sea of the winter and

summer cruises are shown. In general, the summer TCO₂ values are much lower, although in the eastern part of the transect there is an area with only slight differences. We tried to identify the causes of the changes between the winter and summer surface layer in that area in the central Weddell Sea that we visited on both cruises. An outcome was that biological activity contributed most to the observed changes, drawing down the CO₂ concentration in spring and early summer. During winter, vertical transport into the surface layer (Gordon and Huber, 1990) causes the TCO₂ concentration to increase, but this is not enough to cause outgassing of CO₂ at the end of the winter. On the contrary, between our (mid)winter and summer cruises the surface layer must have taken up some CO₂ (Hoppema *et al.*, submitted). Due to the interplay between ice-cover and biology, latter process provokes more CO₂ uptake by the surface layer than it would without ice-cover. Although the Weddell Sea is prone to be a source of CO₂ through upwelling of CDW, the biological pump mechanism

significantly tends to mitigate this effect. Advection out of the Weddell Sea of deep water, which is enriched in CO₂ by this mechanism, makes this whole ensemble particularly effective. This – for CO₂ – the delicate balance between lateral and vertical transports will be the subject of more thorough study. In austral autumn 1996 additional TCO₂ measurements are planned. Then, also the eastern end of the Weddell Gyre will be sampled.

References

- Fahrbach, E., G. Rohardt, M. Schröder, and V. Strass, 1994: Transport and structure of the Weddell Gyre. *Ann. Geophysicae*, 12: 840–855.
- Gordon, A.L., and B.A. Huber, 1990: Southern Ocean winter mixed layer. *J. Geophys. Res.*, C95: 11655–11672.
- Whitworth, III, T., and W.D. Nowlin, Jr., 1987: Water masses and of the Southern Ocean at the Greenwich Meridian. *J. Geophys. Res.*, C92: 6462–6476.

Comparing WOCE and Historical Temperatures in the Deep Southeast Pacific

James H. Swift, Scripps Institution of Oceanography, UCSD, La Jolla, CA 92093-0214, USA

Each WOCE Hydrographic Programme one-time survey section passes near locations of various earlier hydrographic stations, and so we compare WOCE stations to these as we proceed across each section. Differences are to be expected, and when they form a consistent pattern, it makes life at sea a little more interesting.

The research vessel Akademik Ioffe crossed the Amundsen-Bellinghousen Basin in the far Southeast Pacific in early 1992 during a WOCE Hydrographic Programme section along 67°S (S4(P), Ioffe 6/1, M. Koshlyakov and J. Richman; see location in Fig. 1). Temperatures in the Circumpolar Deep Water (1000 to 3000 metres) were often

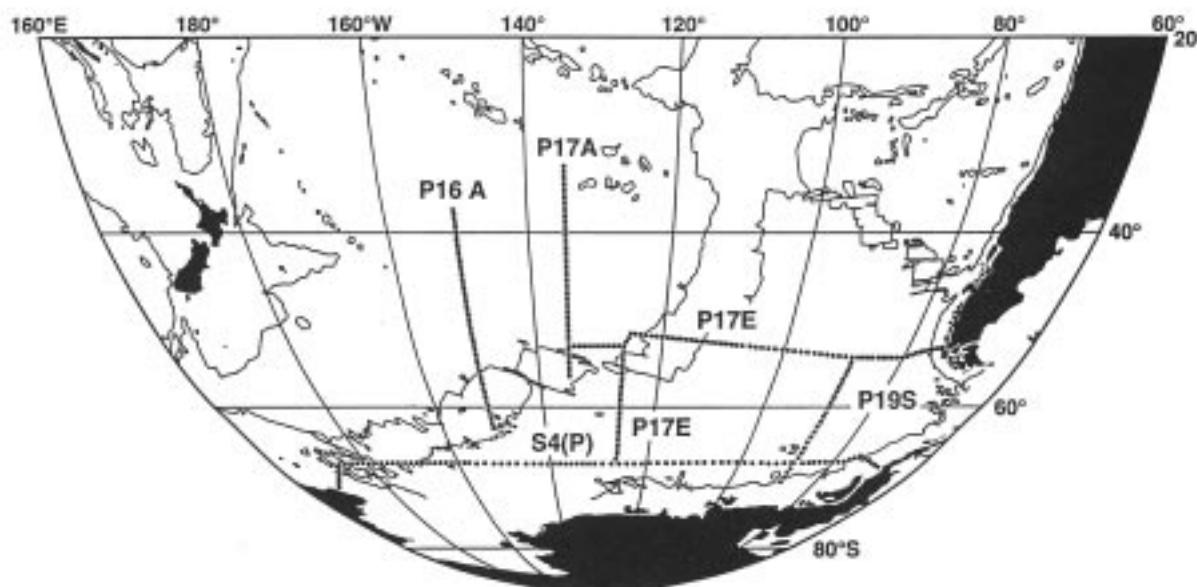


Figure 1. Location of hydrographic stations during Akademik Ioffe 6/1 (S4(P) (67°S); M. Koshlyakov and J. Richman), Knorr 138/9 (P16A (150.5°W), P17A (135°W); J. Reid), and Knorr 138/10 (P17E (126°W and ca. 52°S), and P19S (88°W); J. Swift). P19C data extending north from P19S shown in Fig. 3 were collected by Lynne Talley during Knorr 138/12.

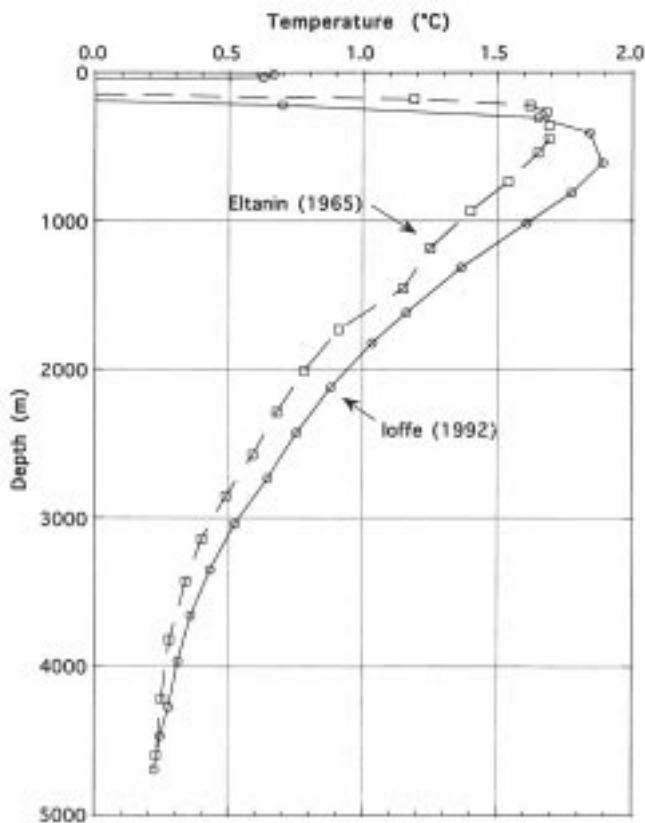


Figure 2. Comparison of temperature profiles near 67°S and 134.5°W from the Ioffe S4(P) line in 1992 with an Eltanin station from 1965.

about 0.05–0.15°C warmer than those observed at overlapping stations from earlier expeditions. For example, Fig. 2 compares an Ioffe station at 67°S, 134.5°W with an Eltanin station from 1965. The Circumpolar Deep Water was clearly warmer at this location in 1992.

One year later RV Knorr ran four WHP sections normal to the Ioffe line. (Knorr 138/9 (J. Reid), and Knorr 138/10 (J. Swift), covering WHP sections P16A (150.5°W), P17A (135°W), P17E (126°W and ca. 52°S), and P19S (88°W). These sections are shown in Fig. 1.) It seemed that many – but certainly not all – of the comparisons carried out with the overlapping earlier data also showed warmer deep water in the recent observations.

This note explores the pattern of the differences and how they most likely arose. Here only the temperature field is examined. Although there are salinity and oxygen data in the historical archives, and these show differences too, the potential for methodological differences to mask real signals is much greater than for temperature, which has been measured to about $\pm 0.02^\circ\text{C}$ in most older data (and much better for WOCE data).

The Pacific–Antarctic Ridge/East Pacific Rise system divides the far South Pacific sector between New Zealand and South America. The principal gaps near the Circumpolar Current waters are the Eltanin and Udintsev fracture zones. The Amundsen–Bellingshausen Basin lies southeast of the ridges, and most of our comparisons are from that region.

We did not sample in the Ross Sea, which marks the far southwestern boundary of the study area.

The principal oceanographic feature, standing out on most mapped isopleths is, of course, the Antarctic Circumpolar Current. Isopycnals in the core of the Circumpolar Deep Water (CDW) and the salinity maximum in that layer slope strongly upward from north to south, from over 3000 m depth at 50°S to the surface in the waters around Antarctica. Olbers *et al.* (1992) found negligible contourable salinity variability in the Amundsen–Bellingshausen Basin on their isopycnal lying closest to the CDW core in their statistically-reduced data, so to first order isopycnals and isotherms are coincident there. The CDW is composed of relatively saline water from the deep North Atlantic – hence the salinity maximum – which has been heavily modified in the Antarctic.

Our WOCE temperature data were compared with gridded data extracted from the data sets compiled by Levitus and by Olbers *et al.* (1992). A single-cruise comparison was possible with an Eltanin section along ca. 90°W with the WOCE data along P19S. The Levitus and Olbers *et al.* data sets are derived from similar station distributions except for the most recent stations and some Russian data included in the latter. Results from comparisons with both were similar, so here we show only the comparison with the Levitus set.

For any WOCE section, we extracted a companion set from the archive and saw to it that both were gridded on matching one-half degree grids. Then it was simply a matter of subtracting one grid from the other and plotting the differences. Auto-contouring was optimised for large-scale (>1 station) features using the same type of tuning used to mimic hand contouring of section data. The study focused almost entirely on the waters in the range 1000–3000 m to avoid seasonal signals in the upper waters and the increasing error in the archive data closer to the bottom (where fewer of the historical data extend). This also fits the early observation that this was the portion of the water column associated with the changes we were trying to document.

We subtracted the historical data from the WOCE data, so positive differences would indicate waters warmer in 1992–93. What we were looking for were consistent patterns of differences between the four meridional sections. For example, if the temperature changes in the range 1000–3000 m were due to a shift in properties of the CDW, then we should expect a coherent difference signal in the core of that water mass, and we should be able to align the four south-north sections by that core and see consistent differences from section to section. But if the temperature changes were due to a shift in the latitude of the axis of the Circumpolar Current, then we should see any resulting differences from section to section best by aligning the four sections by the axis of that current.

As it turned out, the 150.5°W, 135°W, 126°W, and 88°W temperature difference sections did show a great deal of similarity in the circumpolar current axis region. (Here, to save space, we show as Fig. 3 only the 88°W temperature

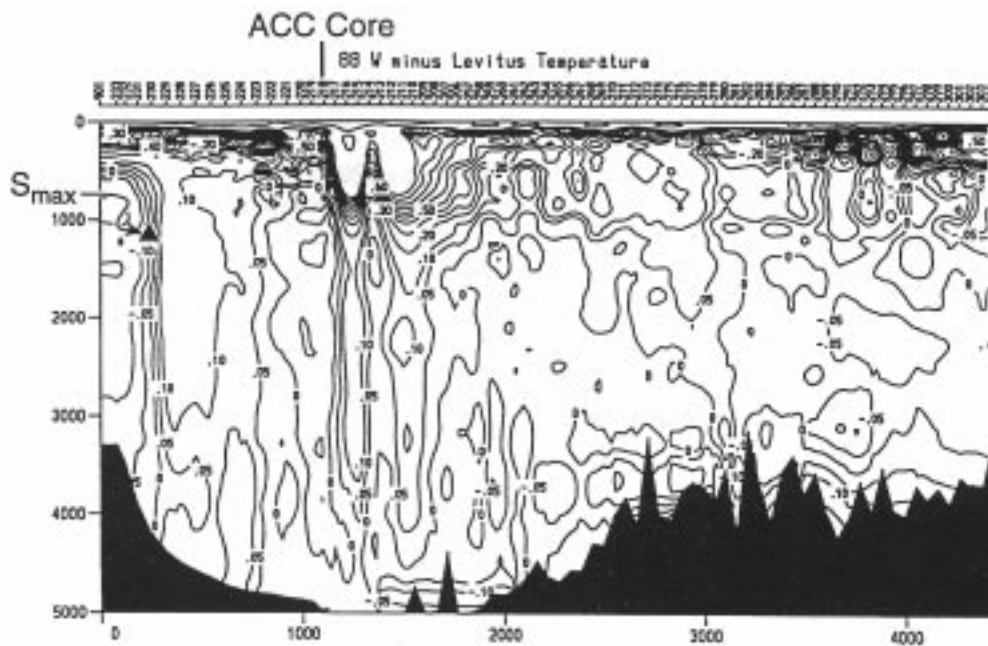


Figure 3. Temperature difference section along P19S (88°W), including some P19C stations as well. The Levitus data were subtracted from WOCE data gridded to the same specification, so positive anomalies show where the water was warmer during WOCE. The strongest feature common to the difference sections for P19C, P17E, P17A, and P16A was the positive anomaly near the axis of the Antarctic Circumpolar Current. The triangle symbol indicates the location of the subsurface salinity maximum on the section, which is one definition of the core of the Circumpolar Deep Water.

difference section.) There was no strong correlation of the differences from all four cross-sections with the core of the CDW. (The deep salinity maximum is found at Station 230 in Fig. 3.) But in almost every case the waters immediately north of the axis of the Circumpolar Current (the axis is near station vertical line in Fig. 3) were warmer during WOCE than earlier.

Because the pattern of differences that was most nearly similar between the four meridional lines – and the strongest – was the positive anomaly associated with the axis of the Circumpolar Current, this suggested that the temperature differences might be partly due to a southward shift of the axis of the Circumpolar Current in the WOCE data as compared to the historical file data. In fact, we could mimic the changes by taking our WOCE data, shifting it north, and subtracting it from itself. The similarities between the WOCE-minus-Levitus and WOCE-minus-shifted WOCE temperature difference sections were remarkable – especially in the 1000–3000 m layer near the axis of the Circumpolar Current. By comparing the south-north lateral temperature gradient in the CDW to the typical temperature changes, we decided that a 50 km (30 minutes of latitude) southward shift could cause the differences in every case. In the Bellingshausen Basin (south end of the 126°W line and south end – up to the slope – of the 88°W line the deep water was an average of 0.04°C warmer during WOCE. The latter was also shown in the Ioffe-Levitus differences along 67°S. This result for the Bellingshausen Basin is consistent with all the single station comparisons we have carried out.

We conclude that in the Southeast Pacific east of the Pacific-Antarctic Ridge there may have been a *ca.* 50 km southward shift in the axis of the Circumpolar Current – or at least in the layer from 1000–3000 m – between the 1960's cruises and WOCE. This shift generates inter-

cruise deep temperature differences near the axis of the Circumpolar Current. We have not yet identified any inter-cruise water mass changes specific to the core of the Circumpolar Deep Water. In other words, the Circumpolar Deep Water did not change in any great way here, just the location of the axis of the current system which carries it. This shift does, however, imply that, compared to the 1960's, during WOCE there was a smaller volume of the Antarctic deep waters south of the circumpolar front in the Bellingshausen Basin.

There was one other robust deep temperature difference not shown in the figures chosen for this note: In the southwest part of the study area (south ends of the 150.5°W and 135°W lines) the deep water was colder during WOCE than in the historical files. This change is not due to a north-south shift in the water masses but is instead a water mass change probably connected to processes in the Ross Sea.

Acknowledgements

The WOCE sea work was carried out with the usual professionalism of the Scripps Oceanographic Data Facility and was greatly assisted by the captains, officers, and crews of Akademik Ioffe and RV Knorr. UCSD student Benjamin Crane carried out much of the computer work, and the gridding/contouring software was provided by Lynne Talley. This work was supported by the US National Science Foundation.

Reference

Olbers, D., V. Gouretski, G. Seiss, and J. Schröter, 1992: Hydrographic Atlas of the Southern Ocean, Alfred-Wegener-Institut, Bremerhaven, 8pp. and 82 plates.

WOCE Observations in the Southern Ocean

N. Penny Holliday, WOCE IPO

The observational tools for studying the Southern Ocean are the same as the rest of the global ocean; hydrographic surveys, subsurface floats, surface drifters, current meters, sea level stations, XBTs and satellites. The following tables and maps summarise which Southern Ocean in situ observations (south of 30°S) will have taken place by the end of the WOCE Intensive Observation Period, and those that will not. Locations of lines, stations and arrays on the maps are approximate and schematic. Low Density XBT sections, and float and drifter deployments are not shown on the maps.

Table 1. WOCE Southern Ocean Observations 1989-1997 (SVS = Small Volume Station)
* indicates section or array does not meet the full WOCE requirements

WHP One-Time Survey Sections

Line	Year	Country	SVS
A11	1993	UK	91
A12/S2	1992	Germany	83
A13	1995	France	104
A14	1995	France	101
A16	1989	USA	41
A17	1994	France	100
A21/S1	1990	Germany	19
A23	1995	UK	110
I6	1995	France	75
I7S	1996	France	53
I8S	1994	USA	73
I9S	1994	USA	65
P7W	1995	Russia	35
P12	1995	Australia	49
P14S	1995	Russia	35
P15S	1996	USA	111
P16S	1991	USA	41
P17S	1992-93	USA	119
P18S	1994	USA	89
P19S	1993	USA	100
S4 (Atlantic)	1996	Germany	80
S4 (Indian)*	1995	Australia	56
S4 (Indian)	1996	USA	107
S4 (Pacific)	1992	Russia	113

Floats

Sector	Year	Country	Floats
Atlantic	1990-93	USA	14
Atlantic	1994-95	USA	25
Indian	1995	USA	30
Pacific	1991-93	USA	48
Pacific	1994-96	USA	30

Drifters

Year	Country	Buoys
1991-93	Australia	24
1991-92	Germany	40
1993-95	South Africa	54
1993-96	USA	390
1994-95	Argentina	8

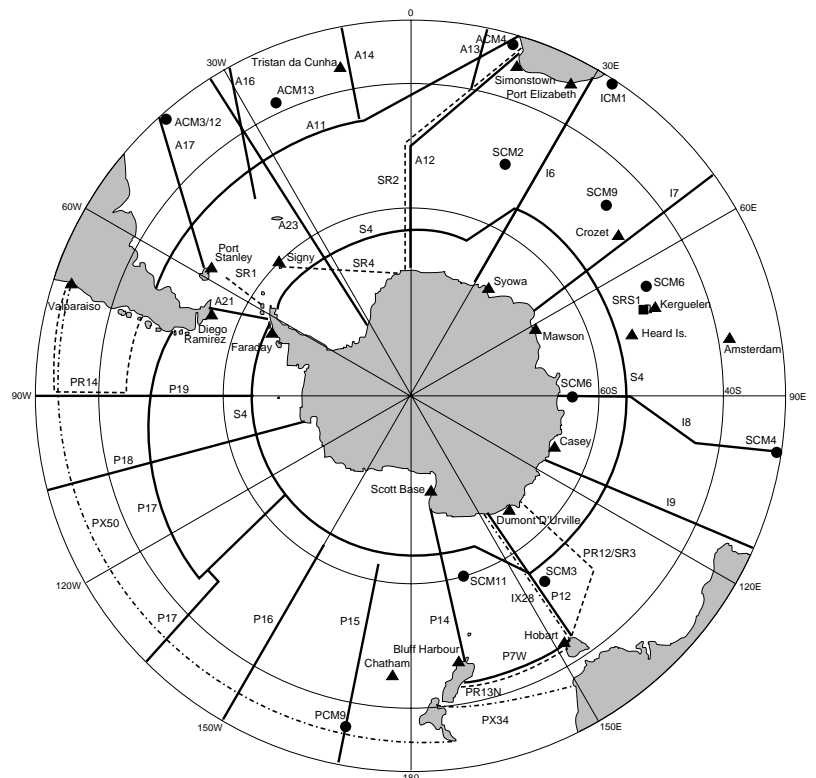
WHP Repeat Sections

Line	Year	Country	SVS per repeat	Rpt
PR12/SR3	1991-96	Australia	49	8
PR13N	1989-94	Australia, NZ	35	6
PR14	1991-94	Chile	25	4
SR1	1992-96	USA, UK, Chile, Spain	14-37	8
SR2	1989-96	Germany, SA	31-83	5
SR4	1989-93	Germany	39-46	4

Time Series Stations

Station	Year	Country
SRS1	1991-96	France

Figure 1. Elements of the Field Programme completed or started by 1997



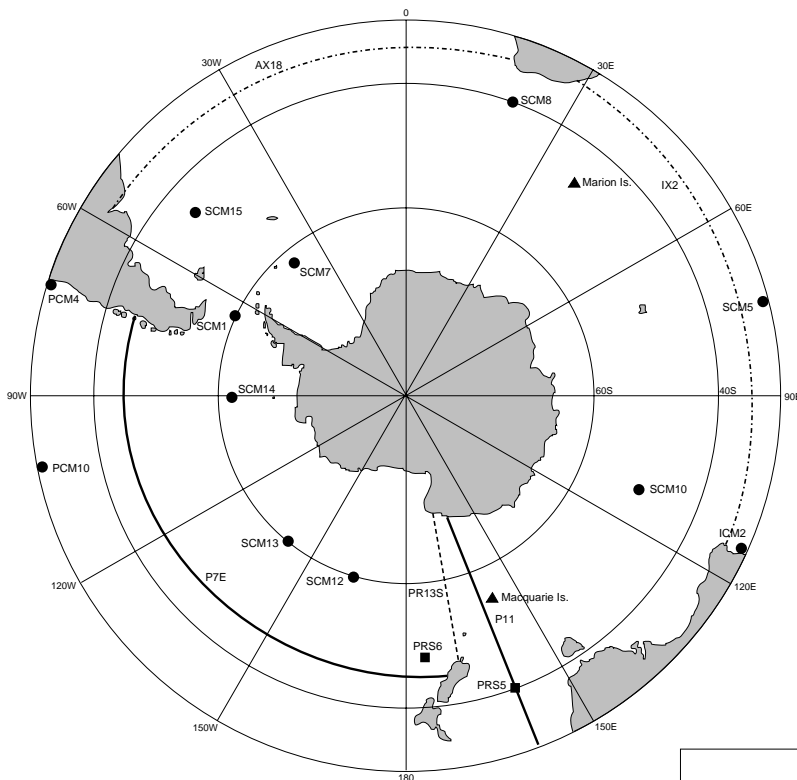
Moored Current Meter Arrays

Array	Year	Country	Mrngs	CMs
ACM3/12	1991-92	Germany	13	59
ACM4	1992-93	USA	4	13
ACM13	1992-94	Germany	6	24
ICM1	1995-96	UK	6	26
PCM9	1991-92	USA/NZ	20	59
SCM2*	1992-95	Germany	2-3	9-14
SCM3	1991-95	Australia	1-4	5-20
SCM4	1995-?	Australia	?	
SCM6	1993-94	UK	15	52
SCM7	1989-93	Germany	7-18	25-64
SCM9	1993-95	UK	8	46
SCM11	No Date	USA	5	15

Sea Level Stations

Station	Year	Country
Bluff Harbour	Ongoing	New Zealand
Casey	Ongoing	Australia
Chatham Is.	Ongoing	New Zealand
Crozet	1995	France
Diego Ramirez	Ongoing	Chile
Dumont D'Urville	1995	France
Faraday	Ongoing	UK
Hobart	Ongoing	Australia
Kerguelen	Ongoing	France
Mar del Plata	Ongoing	Argentina
Mawson	Ongoing	Australia
Port Elizabeth	Ongoing	PSMSL
Port Stanley	Ongoing	UK
Scott Base	Ongoing	New Zealand
Signy	Ongoing	UK
Simonstown	Ongoing	PSMSL
Syowa	Ongoing	Japan
Tristan da Cunha	Ongoing	UK
Valparaiso	Ongoing	Chile

Figure 2. Elements of the Field Programme with no commitment.



- One Time Survey Sections
- - - Repeat Hydrography Sections
- · · High Density XBT Sections
- Moored Current Meter Arrays
- Time Series Stations
- ▲ Sea Level Stations

XBT High Density Lines

Line	Year	Country	Sects
IX28	1995-97	Australia	6
PX34	1991-97	Australia	4
PX50	1993-97	USA	2

XBT Low Density Lines

Line	Year	Country	Sects
AX18	1990-97	Ger, USA	6-12
AX25	1990-91	Germany	intermittent
IX15	1995-97	USA	122
IX21	1995-97	USA	12
IX29	1995-97	Australia	intermittent
PX50	1994-97	USA	12

Table 2. WOCE Southern Ocean Field Programme: Uncommitted Elements

<u>WHP One-Time</u>	<u>Moored CM Arrays</u>	<u>XBT LD</u>
P7E	ICM2	AX22
P11S	PCM4	AX19
<u>WHP Repeat</u>	PCM10	IX2
PR13S	SCM1	IX19
<u>WHP Time Series</u>	SCM5	PX33
PRS5	SCM8	PX34
PRS6	SCM10	PX35
<u>Sea Level Stations</u>	SCM12	<u>XBT HD</u>
Macquarie	SCM13	AX18
Marion Is.	SCM14	IX2
	SCM15	

OCCAM: the Ocean Circulation and Climate Advanced Modelling Project

Peter D. Killworth, NERC Oceanography Unit, Clarendon Laboratory, Parks Road, Oxford OX1 3PU

Twenty years ago ocean modellers had at their disposal one large-scale numerical model, due to Bryan, Cox and Semtner (Bryan, 1969; Cox, 1984). Today this model is still widely used, but other alternatives exist: isopycnic models (Bleck and Smith, 1990; Oberhuber, 1993), sigma co-ordinate models (Haidvogel *et al.*, 1991) and several others. All have advantages and disadvantages, and intercomparisons are the subject of ongoing research (cf. New, 1994). Computer resources are such that these models can now be run at marginally eddy-resolving grid spacings, allowing surprisingly realistic simulations of the world ocean to be produced. Predominant among these are the almost-global $1/4^\circ$ model by Semtner and Chervin (1992), and the current $1/6^\circ$ massively parallel model run at Los Alamos.

As important as actually running these models is the analysis of them: computing time is still a scarce resource. As much effort as goes into the programming and storing of the data needs to be spent on creating suitable ways to understand the physics that emerges from them. To this end, in 1987 the UK decided to create the Fine Resolution Antarctic Model (FRAM), covering one third of the world ocean, and gave most of its attention to how diagnostic efforts would be spread across the community. The initial planning of these efforts thus defined how the model would be set up and run. The project officially ended in 1992, but results from its analysis continue. To date, analysis has concentrated on, *inter alia*:

- the momentum budget of the Antarctic Circumpolar Current (ACC), in terms of:
- z coordinates (Stevens and Ivchenko, 1995), which showed that Reynolds's stress terms were as weak as estimated from data by Johnson and Bryden (1989)
- angular momentum (Döös and Webb, 1994) showing how water moving meridionally (and changing density) can provide the necessary momentum
- isopycnic surfaces (Killworth and Nanneh, 1994), which showed that unlike quasigeostrophic simulations of the ACC, wind stress enters 60% of the fluid layers directly at the surface
- the vorticity budget of the Southern Ocean (Wells and de Cuevas, 1995) which showed that only about 5% of the area satisfied the simple Sverdrup balance
- particle trajectories (Döös, 1995), demonstrating the complex nature of the Conveyor Belt, with particles initially almost coincident ending up in differing ocean basins
- meridional heat fluxes (Saunders and Thompson, 1993; Thompson, 1993) which showed the importance of eddies at the latitude of the Agulhas retroflexion
- topographic interactions: Webb (1993) who modelled the ACC as a response to meridional fluxes in the

presence of island blockings; Killworth (1992) who showed that the Southern Ocean flow was predominantly equivalent-barotropic and hence steered by topography; and Hughes and Killworth (1995), demonstrating that much of the ACC is occupied by flow which essentially vanishes at the bottom, thus relieving the constraint of flow along topography

- comparisons with data: eddy kinetic energy (Stevens and Killworth, 1992); ALACE trajectories (Davis *et al.*, 1995); Agulhas eddy shedding (Lutjeharms and Webb, 1995; Quartly and Srokosz, 1993).

Such models can be (and are!) criticised, primarily for the resolution, which is marginally eddy-resolving at best. For example, analysis of the Community Modeling Effort North Atlantic simulations by Böning *et al.* (1991) shows that eddy energies are very low compared with altimetric estimates, and improving resolution by a factor of two doubles the simulated energy field. Clearly grid spacings are not yet asymptotically small. Nonetheless, these models do provide a vast resource of "data" which modellers and observationalists can call on for data comparison, cruise planning, and so on.

But the hard fact remains that on many occasions the extant models are simply wrong. A notorious example is the separation of the Gulf Stream, which stubbornly occurs far north of Cape Hatteras in almost all North Atlantic simulations. It now seems clear (WOCE-NEG, 1994) that the next step must involve an improvement in model *physics*. Varying the descriptor used for the model (level, isopycnic, *etc.*) is but part of this improvement, since most of the internal physics used in models is unchanged since the 1970s, save for vertical mixing formulations and the like.

In 1992 the UK modelling community bid for an ambitious programme to build a better ocean model. The proposal had eight subprojects: surface fluxes, mixed layers, ice, deep convection and overflows, topography, code improvement, parameterisation of eddies, and a truly global simulation to serve as a testbed for the model improvements. Central funding was available to provide a Core Team to create and run the global model, but the remainder of the project had to be re-bid for individually by PIs. This, inevitably, led to some unfunded subprojects, but contracts with the UK Met. Office have improved this situation, and all subprojects have some activity in progress.

The global model is based originally on the GFDL Modular Ocean Model code. This has been rewritten by Webb (1995a) for use on generic message passing systems. An explicit free surface (Killworth *et al.*, 1991) has been added. The model covers the entire globe, by making use of two co-ordinate grids rather than one. The main grid is

simple latitude-longitude, and covers the world ocean apart from the North Atlantic and Arctic. The second grid is a rotated latitude-longitude grid, with pseudopoles on the equator in the Pacific and Indian Oceans, which permits coverage of the North Pole without the problem of meridian convergence (other methods have been proposed; Bleck, private comm.). The two grids communicate at the equator in the Atlantic (where latitude maps onto the pseudolongitude and vice versa). This method has been tested on known analytical and numerical wave solutions with excellent results (Coward *et al.*, 1994). A new treatment of momentum advection has been added, which removes potential checkerboarding on the B-grid used (Webb, 1995b). Other new features have been developed, but remain to be added to the code. These include a better treatment of tracer advection (Farrow and Stevens, 1995) using the QUICK algorithm, and addition of bottom grid boxes of fractional thickness (Stevens and Maskell, pers. comm.), which removes the long-standing difficulty that the Cox code has needed to have topography “tied” to integral grid point depths.

The model has been coded using Cray-specific shared memory routines, and is now running on the Cray T3D at Edinburgh Parallel Computing Centre, currently with a $1/4^\circ$ resolution, with $1/6^\circ$ planned. An initial spinup of 180 days has been performed, relaxing to Levitus temperature and salinity fields. In the near future a thermodynamic sea-ice code will be added, driven by a simple atmospheric boundary layer model which had been developed for the FRAM sea-ice runs; the choice of ice dynamics has yet to be made. The model will be driven by the NASA Goddard DAO 4D timeseries surface flux fields.

Already in the spinup, strong eddying activity has been seen in the western boundary in the North Atlantic, the Kuroshio, the Agulhas retroflexion, and the Antarctic Circumpolar Current. There is upwelling along the equator, an Indonesian throughflow, a strong eddy off Somalia, upwelling off Arabia and many other features. Predictably, there are minor problems. The Kuroshio is separating from the coast further north along the coast than it should do. The Gulf Stream is separating from the coast at Cape Hatteras but is instantly forming a large meander. However, the point of the project is to work on these difficulties and circumvent them with better physics and numerics.

Fig. 1 shows an example of the surface temperature field at the end of 190 days. Other examples, including small movie simulations and additional information, can be found on World Wide Web under

<http://www.unixa.nerc-wormley.ac.uk>.

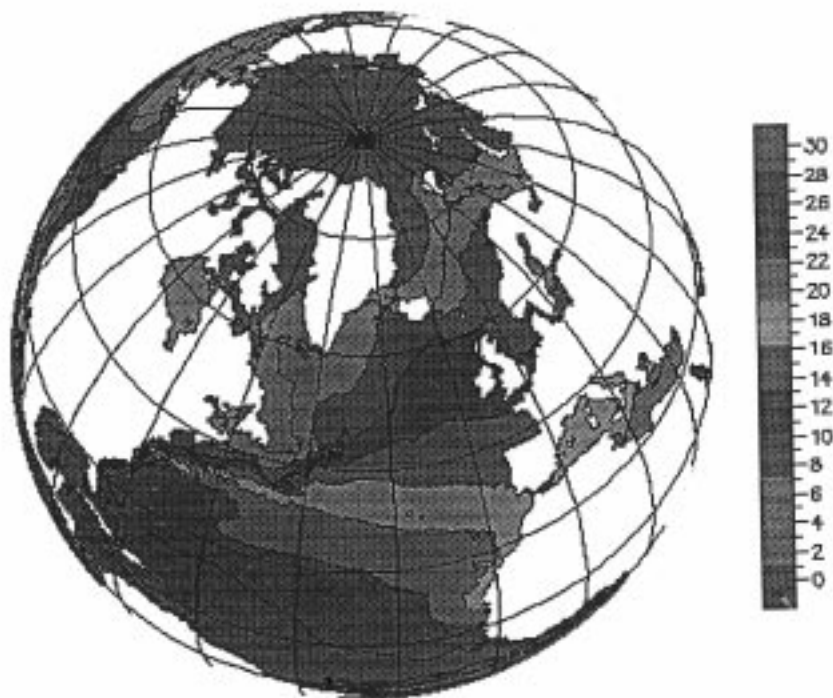


Figure 1. Surface temperature field after 190 days model integration, starting from Levitus annual mean climatology.

References

- Bleck, R., and L.T. Smith, 1990: A wind-driven isopycnic coordinate model of the North and Equatorial Atlantic Ocean. 1. Model development and supporting experiments. *J. Geophys. Res.*, 95, 3273–3286.
- Böning, C.W., R. Döscher, and R.G. Budich, 1991: Seasonal transport variation in the western subtropical North Atlantic: experiments with an eddy-resolving model. *J. Phys. Oceanogr.*, 21, 1271–1289.
- Bryan, K., 1969: A numerical method for the study of the circulation of the world ocean. *J. Comput. Phys.*, 4, 347–376.
- Coward, A.C., P.D. Killworth and J.R. Blundell, 1994: Tests of a two-grid world ocean model. *J. Geophys. Res.*, 99, 22725–22735.
- Cox, M.D., 1984: A primitive equation, 3-dimensional model of the ocean. Technical Report No. 1, Ocean Group, Geophysical Fluid Dynamics Laboratory, Princeton, NJ, USA.
- Davis, R.E., P.D. Killworth and J.R. Blundell, 1995: Simulations of ALACE drifter tracks using the Fine Resolution Antarctic Model. Submitted to *J. Geophys. Res.*
- Döös, K., 1995: Inter-ocean exchange of water masses. *J. Geophys. Res.*, in press.
- Döös, K., and D.J. Webb, 1994: The Deacon Cell and the other meridional cells of the Southern Ocean. *J. Phys. Oceanogr.*, 24, 429–442.
- Farrow, D.E., and D.P. Stevens, 1995: A new tracer advection scheme for Bryan and Cox type Ocean General Circulation Models. *J. Phys. Oceanogr.*, in press.

- Haidvogel, D.B., J.L. Wilkin and R. Young, 1991: A semi-spectral primitive equation ocean circulation model using vertical sigma and orthogonal curvilinear horizontal coordinates. *J. Comp. Phys.*, 94, 151–185.
- Hughes, C.W., and P.D. Killworth, 1995: On the effects of bottom topography in the large-scale circulation of the Southern Ocean. Submitted to *J. Phys. Oceanogr.*
- Johnson, G.C., and H.L. Bryden, 1989: On the size of the Antarctic Circumpolar Current. *Deep-Sea Res.*, 36, 39–53.
- Killworth, P.D., 1992: An equivalent-barotropic mode in the Fine Resolution Antarctic Model. *J. Phys. Oceanogr.*, 22, 1379–1387.
- Killworth, P.D., and M.M. Nanneh 1994: On the isopycnal momentum budget of the Antarctic Circumpolar Current in the Fine Resolution Antarctic Model. *J. Phys. Oceanogr.*, 24, 1201–1223.
- Killworth, P.D., D. Stainforth, D.J. Webb and S. Paterson, 1991: The development of a free surface Bryan-Cox-Semtner model. *J. Phys. Oceanogr.*, 21, 1333–1348.
- Lutjeharms, J.R.E, and D.J. Webb, 1995: Modelling the Agulhas Current System with FRAM (Fine Resolution Antarctic Model). *Deep Sea Res.*, in press.
- New, A.L., 1994: AIM: The Atlantic Isopycnal Model. *International WOCE Newsletter* No. 17.
- Oberhuber, J., 1993: Simulation of the Atlantic circulation with a coupled sea ice-mixed layer-isopycnal general circulation model. Part 1: Model description. *J. Phys. Oceanogr.*, 23, 808–829.
- Quarty, G.D., and M.A. Srokosz, 1993: Seasonal variations in the region of the Agulhas Retroflection: Studies with Geosat and FRAM. *J. Phys. Oceanogr.*, 23, 2107–2124.
- Saunders, P.M., and S.R. Thompson, 1993: Transport, heat and freshwater fluxes within a diagnostic numerical model (FRAM). *J. Phys. Oceanogr.*, 23, 452–464.
- Semtner, A.J., and R.M. Chervin, 1992: Ocean general circulation from a global eddy-resolving model. *J. Geophys. Res.*, 97, 5493–5550.
- Stevens, D., and V. Ivchenko, 1995: The zonal momentum balance in an eddy resolving general circulation model of the Southern Ocean. Submitted to *J. Phys. Oceanogr.*
- Stevens, D., and P.D. Killworth, 1992: The distribution of kinetic energy in the Southern Ocean. A comparison between observations and an Eddy resolving general circulation model. *Phil. Trans. Roy. Soc. B.*, 338, 251–257.
- Thompson, S.R., 1993: Estimation of the transport of heat in the Southern Ocean using a fine resolution numerical model. *J. Phys. Oceanogr.*, 23, 2493–2497.
- Webb, D.J., 1993: A simple model of the effect of the Kerguelen Plateau on the strength of the Antarctic Circumpolar Current. *Geophys. Astrophys. Fl. Dyn.*, 70, 57–84.
- Webb, D.J., 1995a: An ocean model for array processor computers. Submitted to *Computers and Geosciences*.
- Webb, D.J., 1995b: The vertical advection of momentum in the Bryan-Cox-Semtner ocean general circulation model. Submitted to *J. Phys. Oceanogr.*
- Wells, N.C., and B.A. de Cuevas, 1995: Vorticity Dynamics of the Southern Ocean from a General Circulation Model. *J. Phys. Oceanogr.*, in press.
- WOCE International Project Office, 1995: Report of the ninth meeting of the WOCE Numerical Experimentation Group, NEG-9, and 1994 Workshop, Los Alamos National Laboratory, NM, USA, 19-21 September 1994. *WOCE Report No. 125/95*, 24pp.

Early ALACE Results from the Pacific

Russ E. Davis, Scripps Institution of Oceanography, UCSD, La Jolla, CA 92093-0230, USA

The WOCE global survey includes an ambitious subsurface float programme which has the primary goal to measure time-averaged absolute velocity globally on one mid-depth level. This average velocity field could then be used to reference the geostrophic shear fields to be deduced from the post-WOCE hydrographic data set. An additional objective is to observe the time-variable ocean processes which, in the aggregate, form the general circulation and to characterise time variability by calculating eddy energies and time scales and by estimating eddy diffusivities.

The WOCE goal is to obtain five float-years of velocity observations on a single level in every 500 km square of the global ocean. The 500 km scale is roughly the resolution with which it will be possible to map geostrophic shear once the WOCE hydrographic data set is complete. The target of five-year records was based on the anticipated energies and time scales of the variability to be averaged. It was believed that five-year records would reduce the

mean flow uncertainty from mesoscale variability to about 2 mm/s away from boundary currents or 2 cm/s in them. It is hoped, then, that the random sampling achieved by floats over the WOCE observing period would represent the decadal average, say from the 1990 to 2000, that could be combined with geostrophic shear to form input or verification data for models of the quasi-steady modern general circulation.

As part of the one-time WOCE survey, an array of Autonomous Lagrangian Circulation Explorer (ALACE) floats has been deployed near 1000 m depth in the tropical and South Pacific. The ALACE float (Davis *et al.*, 1991) is a Swallow float that drifts at a pre-set depth without being tracked and periodically rises to the surface where it is located by, and transmits data to, System Argos satellites. In the Pacific survey most ALACEs surface every 26.5 days and were expected to have a power-limited life of 60 cycles or roughly 4.5 years. The floats are tracked during

their 24-hour surface intervals so that while surface drift destroys any pretext of following a specific water parcel, it introduces only random errors of the order 3 km into the subsurface displacement. This uncertainty, roughly equivalent to the accuracy of long-range acoustic tracking, translates into a random velocity noise of the order 1 mm/s in each 25.5-day average velocity. Thus the primary cause of errors in estimated mean currents comes from temporal variability, not the surfacing cycle of ALACE's operation. The 1000 m operating depth was selected as a balance between extending the energy-limited ALACE lifetime and operating below the most vigorous mesoscale variability that confuses averaging.

Because they require no tracking array, ALACEs are well suited to the low-density arrays required for the WOCE float plan that calls for 1100 records of 5-year duration over the globe. For the same reason, ALACEs are logistically attractive in situations like the global survey where floats are widely dispersed and long records are required. Because they are untracked for extended periods, ALACEs cannot map spatial structures on the mesoscale but they can, nevertheless, characterise eddy statistics and dispersion.

Since 1991 some 275 ALACEs have been deployed in the Pacific south of about 30°N; over 180 are still in service and at least 8 more will be deployed this year. It is too early to attempt a comprehensive analysis or to begin integration with the hydrographic observations. The purpose of this note is to report some preliminary results from the Pacific survey that describe

- (a) how well ALACE has performed,
- (b) what the observed time variability implies about the accuracy with which mean currents will be measured with the full data set, and

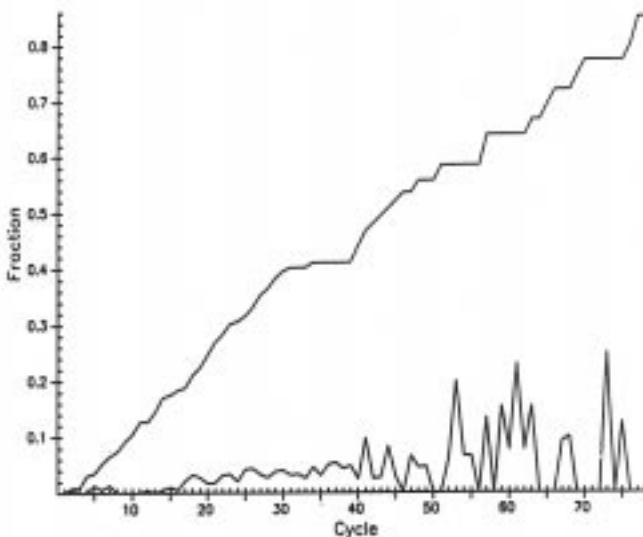


Figure 1. Failure rate of all ALACEs deployed in 1990 through 1993. Upper curve is fraction that have failed vs. number of scheduled cycles. Lower curve is fraction of scheduled surfacings for which operational floats are not located by Argos.

- (c) what can be learned about mean flow in some of the better sampled parts of the survey.

ALACE operation has not been trouble-free. Indeed since the first significant deployment in Drake Passage in early 1990 we have introduced a sequence of substantial design improvements into the float and an even larger number of improvements have been made in quality control by the manufacturer Webb Research Corporation. These have improved reliability and today we are able to deploy most floats with normal checkout and preparation. Early floats were not anodised and were subject to significant corrosion which we believe to have caused frequent slow drifts in float depth and some sudden failures. Since floats have been anodised, slow drifts of depth are rare and there is no sign of the pressure case creep implicated in the slow deepening of early SOFAR floats.

Fig. 1 shows the fraction of floats that have failed vs. number of cycles (most are 26-day cycles). This curve shows a remarkably uniform failure rate, not at all what would be expected from energy exhaustion failures or even from corrosion. We believe this moderate but uniform failure rate results from failures of the hydraulic pump which is used well outside its design operating envelope. New pump designs are under test. Even though only 45% of the floats achieve a 50 cycle life, the total number of cycles completed by a large number (N) of floats has to date been approximately 50 times N.

Fig. 2 shows all the ALACE trajectories in the Pacific observed through December of 1994. In this depiction of raw data, submerged displacements over 25.5 days are plotted as arrows separated by gaps that represent the on-surface drift. This figure is useful primarily to show the density of observation which, at this time is only about 25% of the WOCE goal. It is not even possible to detect current strength from the length of the plotted trajectories because the duration since deployment varies markedly over the array.

One qualitative feature is, however, evident even in Fig. 2. Within about 25° of the equator float displacements are largely zonal with little net meridional motion. While there is little meridional motion, the flow is neither steady nor are there obvious patterns of large-scale spatial coherence to the variability. The float motion in this zone is qualitatively different from the behaviour seen in SOFAR float observations in the mid-latitude North Atlantic reported by Rossby, Webb, Richardson and others. Based on a much denser array of intermediate-depth RAFOS floats in the western North Pacific, Riser (1995) also reports that the flow is dominated by zonal structures. At this point this is simply a qualitative observation that may or may not be an important clue to interior ocean dynamics and possibly to a qualitative difference between the Atlantic and Pacific that can be explained.

Within 10° of the equator, time variability swamps mean motion in the central ocean. The ALACE sampling density is yet inadequate to well describe this variability. Its time scale is of the order one year but does not seem to be associated with the seasonal cycle. Speeds range from

5 to 8 cm/s averaged over several months. The meridional scale is too short (<200km) to be unambiguously determined from the observations. The zonal scale appears to be several thousand kilometres but this is difficult to quantify because the meridional scale is short and two floats are rarely at exactly the same latitude. The temporally-lagged structure functions of velocity (not shown) disclose a marked difference between the time scale of zonal flows within 10° of the equator and those of either equatorial meridional flows or variability outside the tropics. Again, existence of this vigorous quasi-annual zonal variability is now simply a qualitative observation that needs to be explained. It is likely to be related to the slowly varying deep zonal jets reported by Firing (1987). Qualitatively similar features are observed in the eddy-resolving ocean general circulation model described by Semtner and Chervin (1992), but to date all attempts to relate details of simulations and observations have failed.

If one imagines what Fig. 2 will look like when the relatively recent deployments, particularly those on P18 (110°W) and P21 (20°S), have contributed several years of data, it is possible to estimate how well the WOCE sampling goal will be approached. The region from 60°S to 20°N in the Pacific corresponds to more than 400 squares that are 500 km on a side. Thus even if the ALACEs yield an average of 5 record-years, the 275 deployed floats will fall somewhat short of the WOCE goal. Aside from the obviously inadequate sampling north of 20°N, there are a number of thin points in the array. The gap along 125°W will likely be filled somewhat by floats from P18 and the whole southeast of New Guinea will likely gain some

coverage from floats now farther to the southeast. The most seriously undersampled areas would appear to be the southern Tasman Sea and the Southwest Pacific Basin southeast of New Zealand. Additional floats to be deployed into the Tasman Sea this spring should help in this region where variability is large and scales small. The area southeast of New Zealand is shielded from deployments in the Antarctic Circumpolar Current (ACC) by Campbell Plateau so that a deployment directly into the region will be required. Suitable deployment vessels are being sought.

While it is too early to attempt a comprehensive analysis, the results in Fig. 2 already define the low-frequency circulation in the better sampled portions of the tropical and South Pacific. Fig. 3 shows area-average velocities computed from floats deployed before 1994. The areas used to establish these Eulerian averages were selected to be between 500 and 1000 km in dimension and to give between 3 and 7 years of data while encompassing natural clusters of floats and reflecting the probable effects of bottom topography. The areas overlap only a little. A total of 4793 displacements over a total of 336 years were used to construct the averages shown. (Much of the data lost in the area-averaging process when the float density is too low to provide enough samples in a 1000 km square.) Sampling error ellipses are based on measured variances of displacements and the assumption that successive displacements are uncorrelated. This estimate fairly measures the error produced by mesoscale variability but not the quasi-annual variability that dominates within 10° of the equator.

Fig. 3 discloses a number of features anticipated from

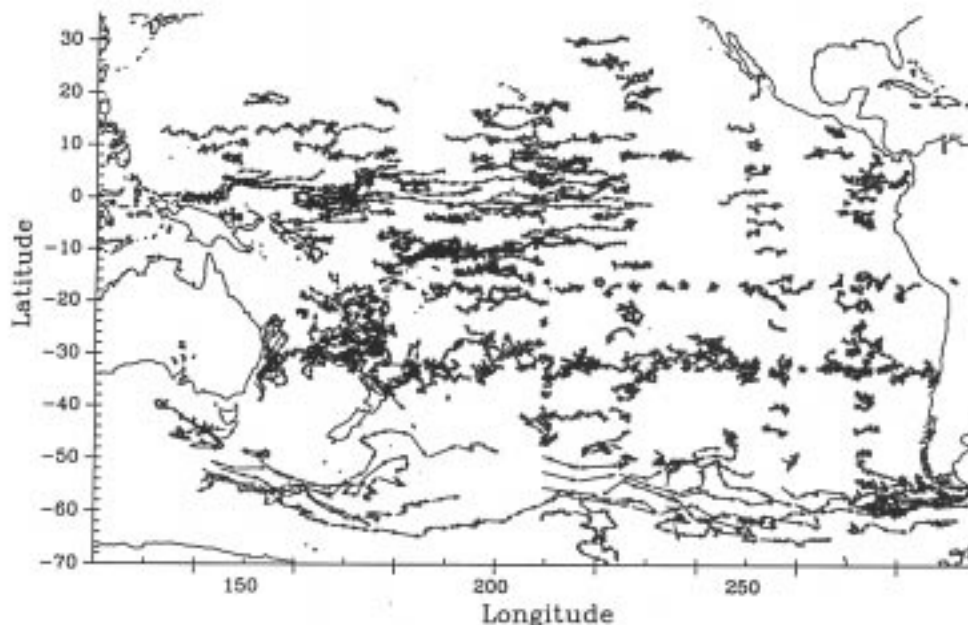


Figure 2. Trajectories of all Pacific ALACEs deployed from June 1991 through December 1994. This is intended to show float coverage at the nominal depth of 1000 m. Each plotted trajectory consists of arrows showing underwater displacement separated by gaps that represent on-surface drift. Motion is difficult to define in the plot except in the Antarctic Circumpolar Current.

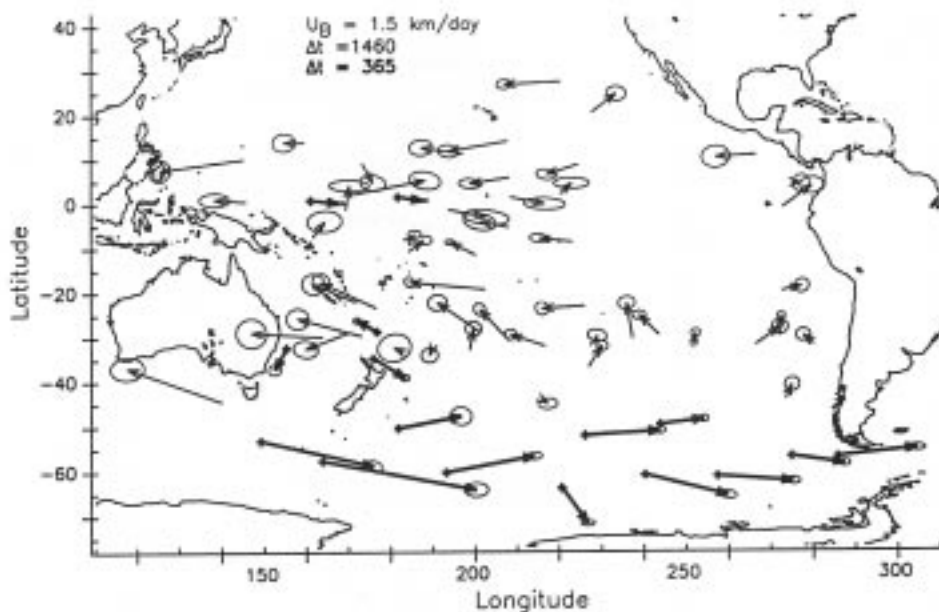


Figure 3. Area-averages of ALACE velocities near 1000 m depth. Light arrows are the displacement over 4 years associated with mean currents of $< 1.5 \text{ km/day}$. The vector base is at the average position of the float velocities averaged. Thick arrows with a plus at their base represent the displacement by mean currents with speeds $> 1.5 \text{ km/day}$. This figure is based on 4793 displacements (most over 25.5 days) spanning 336 float-years. The diameter of the plotted ellipses represent the sampling error on these averages estimated by assuming the correlation time scale is less than one cycle. In the tropics this does not represent the uncertainty introduced by zonal flows with order one-year time scales.

hydrography. The ACC stands out with mean velocities of 6 cm/s south of New Zealand to 4 cm/s approaching Drake Passage. The counter flow south of Australia is slower (about 1.5 cm/s) but unambiguous. The northward invasion of water across 30°S east of 160°W is weak but consistent. Northward mean velocities in this area range from 1 to 4 mm/s with an area average near 2 mm/s. Since the floats are only slightly deeper than Antarctic Intermediate Water (AAIW), this broadscale flow presumably represents invasion of AAIW into the South Pacific. As our estimates of large-scale currents become more accurate it will be possible to determine the velocity of this invasion with errors less than 1 mm/s, to accurately determine the transport of AAIW, and possibly to identify if there are specific areas where it occurs preferentially. Coupled with WHP observations and historical hydrographic data, these observations can be extended to all depths where the mean flow is geostrophic.

Between 30°S and 10°S the floats chart a generally westward flow which, in the western regions, approaches velocities of 1 cm/s. Because of inadequate spatial resolution the picture in the Tasman Sea is incomplete but includes a moderately clear indication of a southward East Australian Current with speeds approaching 2 cm/s. A comparable boundary current also appears to exist along the northeast coast of New Zealand's North Island.

The pattern of broad westward flow between 10 and 30°S appears to be repeated in the northern hemisphere although the data is much sketchier. The picture in the tropics is much more confused. This probably results from two effects. First, it is likely that the meridional scales of the mean flow become short near the equator. Second, whatever mean flow may exist is confused by the vigorous zonal variability with quasi-annual time scales. There is a

suggestion of northward flow across 10°S in the west. Flow within 5° of the equator is highly zonal, occasionally strong, and frustratingly chaotic in direction. Sorting out this behaviour will likely depend on (a) additional sampling over the next few years and (b) discovering the nature of the quasi-annual zonal variability so that it can be removed by coherent filtering.

The area averaging procedure used to develop Fig. 3 is primitive and suitable only for preliminary analysis. In a recent analysis of the first ALACE deployment in Drake Passage (Davis *et al.*, 1995), objective mapping was found a more successful way of extracting patterns of mean flow from the random space-time array provided by float sampling. In this procedure flow divergence can be limited using quasi-geostrophy or potential-density conservation and observations of the thickness of layers defined by potential density.

While the primary goal of ALACE deployments in WOCE has been to map large-scale low-frequency currents, we are now trying to exploit ALACE's vertical cycling to gather profiles of upper ocean temperature and salinity. Particular emphasis has been placed on gathering winter data from high latitude regions where air-sea interaction has the greatest impact on the deep ocean yet winter observations are rare. A few of the floats in the eastern part of the Southern Ocean in Fig. 2 report temperature profiles from 1000 m roughly once per month. In the Atlantic, under NOAA sponsorship, a number of Profiling ALACES (PALACES) have been deployed primarily to report temperature and, in some cases, salinity profiles. Of particular interest in planning for the forthcoming WOCE examination of the North Atlantic, six PALACES (including two that measure salinity profiles) were recently deployed near 1500 m depth in the southern Labrador Sea and

northern Irminger Basin. These were deployed by John Lazier from the Meteor this November. While it is too early to report results from these deployments, this may be a useful pilot experiment for WOCE attempts to monitor the Atlantic Subarctic gyre using floats.

References

- Davis, R.E., P.D. Killworth, and J.R. Blundell, 1994: Comparison of ALACE and FRAM results in the South Atlantic. *J. Geophys. Res.* (submitted).
- Davis, R.E., D.C. Webb, L.A. Regier, and J. Dufour, 1991: The Autonomous Lagrangian Circulation Explorer (ALACE). *J. Atmosph. Oceanic Techn.*, 9, 264–285.
- Firing, E., 1987: Deep zonal jets in the central equatorial Pacific. *J. Mar. Res.*, 45, 791–812.
- Riser, S.C., 1995: New Lagrangian measurements of the flow filed at mid-depth in the western North Pacific. Abstract of talk to be given to IAPSO, August 1995.
- Semtner, A.J., and R.M. Chervin, 1992: Ocean general circulation from a global eddy-resolving model. *J. Geophys. Res.*, 97, 5493–5550.

RAFOS Floats in the Antarctic Intermediate Water of the South Atlantic

Olaf Boebel and Claudia Schmid, Institut für Meereskunde, Universität Kiel, 24103 Kiel, Germany

The Antarctic Intermediate Water

The Antarctic Intermediate Water (AAIW) extends from the subtropical South Atlantic into the North Atlantic reaching as far north as 20°N. It is found at latitude dependent core depths ranging from 700 m to 900 m and may be distinguished from the Central Water above and the North Atlantic Deep Water below by its distinctive salinity minimum and oxygen maximum. The site of formation is supposedly close to the Polar Front, but the import of AAIW through the Drake Passage from the Southeastern Pacific is also a possibility (McCartney, 1977). The possible pathways of the AAIW to the North at intermediate latitudes in the South Atlantic have been studied to a great extent. Reid (1989) discussed both the idea of a continuous flow of AAIW along the western boundary, as suggested by Wüst (1935), and the possibility of an anticyclonic flow underneath the subtropical anticyclonic gyre. According to Taft (1963) and Buscaglia (1971) AAIW would then depart eastward from the western boundary around 40°S and return to the western continental shelf at 25°S. However, no direct observations proving such a subtropical recirculation cell existed to date.

The description of the advection of the AAIW is the major research objective of the IfM Kiel 'RAFOS float' project in the South Atlantic. The project is incorporated in the Deep Basin Experiment (Hogg, 1994) in the framework of the WOCE Core Project 3.

RAFOS floats

RAFOS floats are well suited to explore the drift of this water mass. These Lagrangian drifters float freely at a predetermined depth. They house a microcomputer that determines the float's position by acoustic tracking and measures pressure (p) and temperature (T) once a day. The acoustic tracking is achieved by measuring the times of

arrivals (TOA) of coded sound signals transmitted by moored sound sources. The data quintuplet (p,T,3xTOA) is stored and subsequently transmitted to Kiel through the ARGOS satellite system, once the float has returned to the sea surface. The underwater mission may last for up to two years. Trajectories obtained so far from 17 floats (Fig. 1) launched during Meteor cruise 22 (M22) show a mean flow

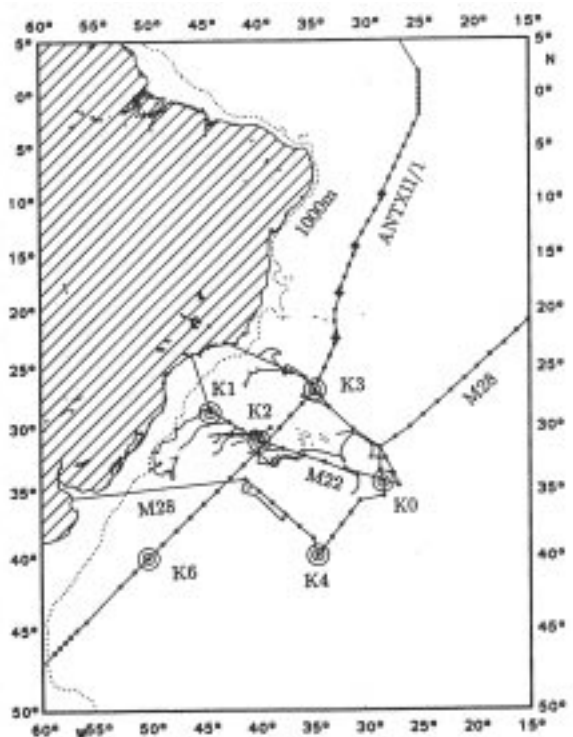


Figure 1. Western South Atlantic with 1000 m isobath (dashed line). Solid curves: float trajectories launched during M22. Open circles: sound source positions. Asterisks: launch positions of floats. M22 (12/1992), M28 (5/1994), ANT XII/1 (11/1994).

of 5 cm/s in predominantly western directions between 25°S and 32°S. Data obtained by R. Davis farther south using Autonomous Lagrangian Current Explorer (ALACE floats), however, depict a strong eastward flow at 40°S. Thus, for a working hypothesis, the assumption of the centre of a recirculation cell of AAIW at 36°S is reasonable and was used for the determination of the sound source position and float deployment pattern during the Meteor cruise 28 (M28) and the Polarstern cruise ANT XII/1.

The Polarstern cruise ANT XII/1

During the Polarstern cruise ANT XII/1 from Bremerhaven to Punta Arenas in November 1994 the last of three RAFOS float seedings in the area was performed by IfM Kiel. During the previous expeditions M22 (December 1992) and M28 (May 1994), 23 and 29 floats were seeded, respectively (Fig. 1). During ANT XII/1 a total of 42 RAFOS floats were deployed, one at every degree of latitude, covering the western South Atlantic from the equator to 39°S. The floats were programmed to mission lengths ranging from 361 days (1 year) to 721 days (2 years). This results in a total of 52 float years or an average under-water mission length of 14.8 month per float. A total of 43 CTD casts were taken during ANT XII/1 to determine the depth of the AAIW core. This information was used to individually ballast each float to reach neutral buoyancy at the depth of the salinity minimum of the AAIW (Fig. 2).

The CTD was used in conjunction with a 24-bottle (10l each) rosette sampler to draw water from different water masses in order to provide the organic (G. Kattner,

AWI, Bremerhaven) and inorganic chemists (J. Butler, NOAA, Boulder) on board with samples. At 7 stations, deep hydrocasts were taken to at least 3000 m. The majority of the casts however, were terminated at 1500 m, after covering the AAIW layer. Fig. 2 shows the salinity section obtained from raw data. One can clearly observe the salinity minimum of the AAIW ranging from 40°S to 20°N. The AAIW tongue ceases at 20°N where it faces high salinity water from the North. At 40°S a possible formation area of AAIW is indicated by an outcrop of isohalines. Here, the lowest salinities during the whole cruise were observed. The salinity minimum of the AAIW rises slowly from approximately 950 dbar at 37°S to 700 dbar at the equator.

In addition to the Kiel RAFOS floats, 8 ALACE floats were launched for R. Davis, R. Peterson and W. White (Scripps Institution of Oceanography) south of 40°S. These instruments operate independently of sound coverage by cycling between surface and drifting depth on a 10 day schedule. Thus, the area observed by drifters is extended southward into the Falkland Current. Furthermore, 29 MARVOR floats seeded during this cruise by M. Ollitrault and his group (IFREMER, Brest) will improve the knowledge of diffusivity and advection in the area. These floats were seeded between 2°N to 2°S crossing the equator at 25°W and in four batches of five floats, arranged in a cross pattern of about 40 km side length to study diffusivity. These instruments actively ballast themselves to approximately 800 dbar. To observe the motion of the thermocline water, surface drifters drogued at 100 m were provided by W. Krauss (IfM, Kiel). On a number of previous expeditions

a total of 150 drifters were deployed in the South Atlantic. During this cruise, additional 35 drifters were seeded between 2°S and 46°S at positions uncovered so far by surface drifter trajectories.

Finally, the existing sound source array was extended to the South. During M22, four sound sources (K0-K3) were deployed around the Rio Grande Rise in addition to an American sound source array deployed farther north in the Brazilian Basin. During M28 K0 was replaced and IfM Kiel added another in the western Argentine Basin at 40°03.14S 50°08.54W (Fig. 1) and enlarges the area covered by sound signals to the

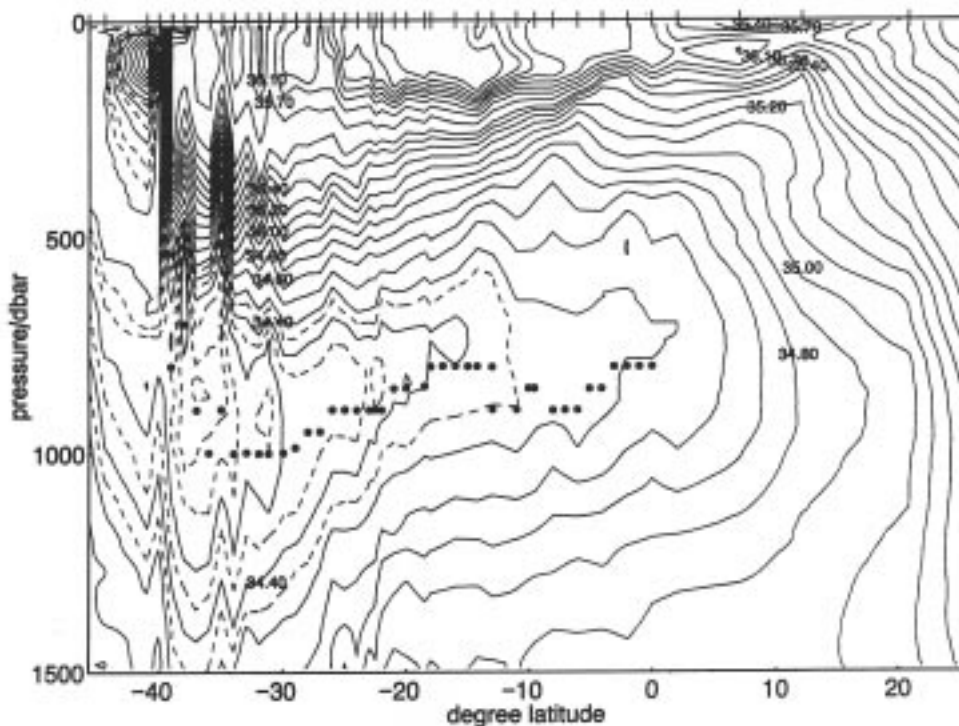


Figure 2. Section of salinity based on preliminary data, obtained by CTD-casts taken during ANT XII/1. The bullets represent launch positions of RAFOS floats at their target depth.

South in order to track floats caught in the recirculating branch of the AAIW.

Acknowledgement

With pleasure we acknowledge the technical assistance of U. Huenninghaus and P. Meyer in the preparation of the floats. The officers and crews of FS Polarstern substantially contributed to the success of this project. We appreciate the support of Deutsche Forschungsgemeinschaft (DFG) and the Bundesministerium für Forschung und Technologie (BMFT).

References

- Buscaglia, J.L., 1971: On the circulation of the Intermediate Water in the southwestern Atlantic Ocean. *J. Mar. Res.* 29, 245–255.
- Hogg, N., 1994: Status of the Deep Basin Experiment. *Intern. WOCE Newsl.* 17, 5–6.
- McCartney, M.S., 1977: Subantarctic Mode Water. In: *A voyage of Discovery*, edited by M. Angel, 103–119.
- Reid, J.L., 1989: On the total geostrophic circulation of the South Atlantic Ocean: Flow patterns, tracers and transports. *Progr. Oceanogr.*, 23, 149–244.
- Taft, B.A., 1963: Distribution of salinity and dissolved oxygen on surfaces of uniform potential specific volume in the South Atlantic, South Pacific, and Indian Oceans. *J. Mar. Res.*, 21(2), 129–146.
- Wüst, G., 1935: Schichtung und Zirkulation des Atlantischen Ozeans, Die Stratosphäre. In: *Wissenschaftliche Ergebnisse der Deutschen Atlantischen Expedition auf dem Forschungs- und Vermessungsschiff "Meteor" 1925-1927*, 6. Lieferung 1. Teil, 2, 180pp. (The stratosphere of the Atlantic Ocean, W.J. Emery, editor, Amerind Publishing, New Delhi, 112pp, 1980).

Meridional Transport Estimates for the Northern North Atlantic

Manfred Bersch and Jens Meincke, Institut für Meereskunde, Universität Hamburg, 22529 Hamburg, Germany

On Meteor cruise 18 between 2 and 22 September 1991 two sections with hydrographic and current measurements were run from Reykjavik to Cape Farvel at the southern tip of Greenland and from Cape Farvel to the Porcupine Bank off the Irish coast (WOCE section A1E/AR7E). The continuous current measurements were performed with a ship-mounted Acoustic Doppler Current Profiler (ADCP) with a transducer frequency of 153.6 kHz, reaching a maximum depth of about 450 m. The ADCP data, sampled during intervals of 4 minutes, were corrected

for the ship velocity, misalignment and scaling effects, and tidal motion. Temporal averaging between pairs of CTD stations increases the accuracy of the derived velocities from about 30 cm/s for a single profile to about 3.6 cm/s for a section segment.

Fig. 1 shows the horizontal structure of the derived flow field of the upper 500 m along both sections. West of the Reykjanes Ridge, in the Irminger Sea, the highest velocities of about 20 cm/s are associated with the East Greenland Current, following the isobaths of the continental

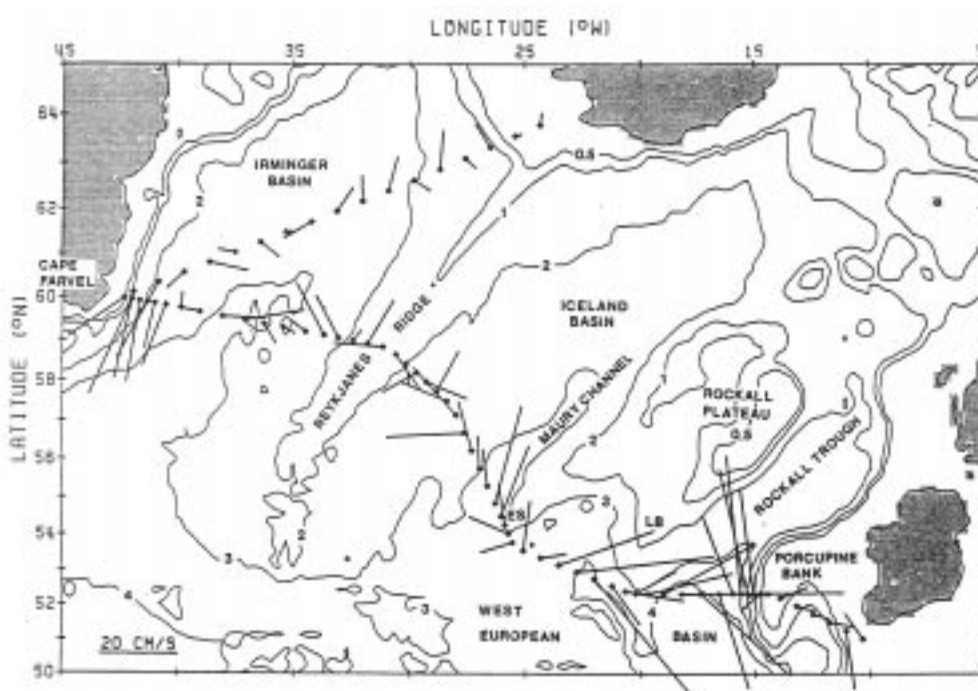


Figure 1. Geographical distribution of the corrected water velocity from ADCP measurements along the Greenland-Iceland and Greenland-Ireland sections, averaged horizontally (between the CTD stations on the southern section) and between 70 and 350 m depth. The bases of the velocity vectors are marked by dots. Bottom topography is in km. ES: Eriador Seamount, LB: Lorient Bank.

slope off Greenland. Enhanced northward velocities of 10 to 15 cm/s on both sections indicate the location of the Irminger Current above the western slope of the Reykjanes Ridge. There is only a weak southward flow of the Irminger Current above the eastern slope of the ridge, near the 2000 m isobath. At about 24°W a divergence occurs in the North Atlantic Current, encountering the Rockall Plateau. The northern branch, representing the Irminger Current, passes the Eriador Seamount to the west and enters the Iceland Basin above the Maury Channel with speeds of about 25 cm/s. The southern branch of the North Atlantic Current follows the isobaths of the Lorien Bank in cyclonic sense with speeds of up to 40 cm/s and enters the Rockall Trough at its western side. The strongest northward flow with a speed of 35 cm/s is found above the 2000 to 3000 m isobaths of the slope of the Porcupine Bank. Near the axis of the Rockall Trough the ADCP data indicate a relatively strong southward flow.

Along the Greenland-Ireland section the water column has a three-layer structure (Fig. 2). The upper layer is occupied by relatively warm and saline Subpolar Mode Water (SPMW) with some colder and fresher intrusions of Subarctic Intermediate Water in the eastern part of the Iceland Basin. In the mid-depth layer Labrador Sea Water (LSW) characterized by a salinity minimum extends along the whole section. The bottom layer contains relatively saline Iceland-Scotland Overflow Water (ISOW) on both flanks of the Reykjanes Ridge, less saline Lower Deep Water (LDW) at the entrance of the Rockall Trough, and less saline Denmark Strait Overflow Water (DSOW) in the Irminger Basin.

Geostrophic Velocities

The geostrophic velocities, calculated from the hydrographic data, were fitted to the ADCP velocity components perpendicular to the section between 70 and 350 m depth, which are considered as representative of the geostrophic flow across the section in this depth interval. The accuracy of the derived velocities is comparable to that using a layer of no motion in the geostrophic calculations.

The structure of the ADCP

referenced geostrophic flow field is essentially columnar without any pronounced layer of no motion (Fig. 3). The distributions of velocities and water mass characteristics indicate cyclonic circulations above the Irminger and Iceland basins and an enhanced deep-reaching mesoscale variability near the Rockall Plateau and in the Rockall Trough. A northward flow of recently formed LSW, which is accompanied by less saline water in the upper layer, occurs at about 1500 m depth at 39°W in the Irminger Sea. There is no pronounced bottom intensification of the southward flow of ISOW along the eastern flank of the Reykjanes Ridge and only a weak northward flow of ISOW, which has entered the western Atlantic through the Charlie-Gibbs Fracture Zone, in the Irminger Sea. Above the continental slope off Cape Farvel the southward flow exhibits two current cores with speeds above 25 cm/s. While the upper

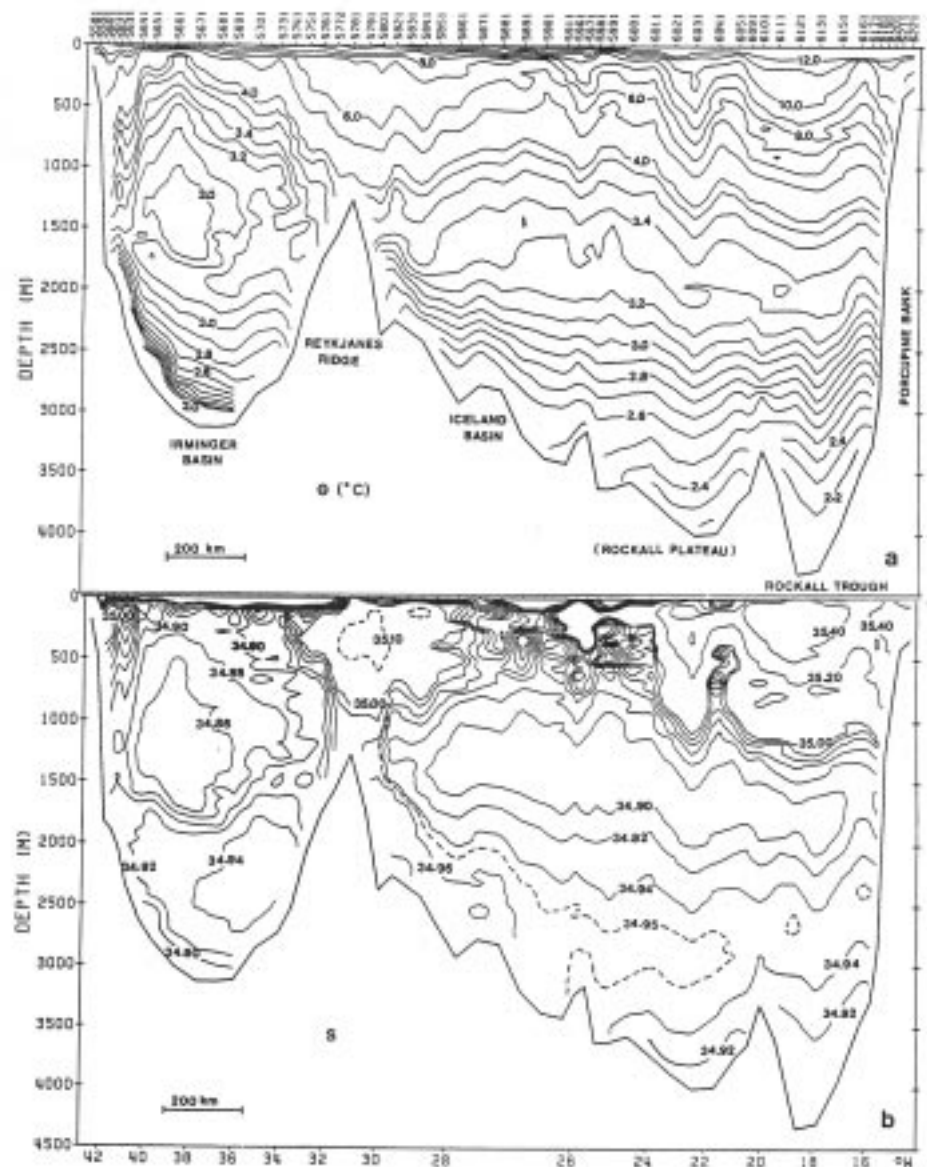


Figure 2. Vertical distributions of potential temperature (a) and salinity (b) along the Greenland-Ireland section.

is associated with the front between the relatively cold and less saline Arctic waters, found on the shelf and near the shelf break, and the SPMW farther downslope, the lower is related to the DSOW and occurs near the 2200 m isobath. The two-core structure of the flow above the slope near Cape Farvel is also described by Clarke (1984) from hydrographic and current measurements.

Transports

From the geostrophic flow field referenced to the ADCP velocities volume transports were calculated. The total transport through the Greenland-Ireland section is -16 Sv (negative values indicate southward transports). It is adjusted to the expected balance of about zero by applying a velocity correction of 0.27 cm/s, which is within the accuracy of the misalignment estimation. The heat and salt balances for the adjusted section yield net northward transports of 0.49×10^{15} W and 1.1×10^7 kg/s, respectively, which are comparable to estimates by Krauss (1986).

The regional and vertical distribution of the calculated volume transports is shown in Fig. 4 with corresponding estimates of the accuracy. The upper two layers are separated by $\sigma_0 = 27.72$ kg/m³, the lower two layers by $\sigma_0 = 27.80$ kg/m³. From the top to the bottom the net transports of the three layers are 15 Sv, -3 Sv, and -12 Sv (negative values: southward). Compared to Schmitz and McCartney (1993), who report transports of 6 Sv, 3 Sv, and -9 Sv, respectively, an increased net northward transport of SPMW across the line Cape Farvel to Porcupine Bank and an increased entrainment of SPMW into the LSW (3 Sv) and the overflows (6 Sv) are suggested. The entrainment has the same order of magnitude as the formation rates of the LSW or the overflow waters. Only about one third of the subtropical supply of SPMW of about 20 Sv is converted to deep water in the Nordic Seas, the other two thirds are converted in the subpolar gyre. About 7 Sv of SPMW enter the Rockall Trough and probably flow through the Faeroe-Shetland Channel, where Gould *et al.* (1985) calculated an annual mean transport of 7.8 Sv from current meter measurements, into the Norwegian Sea. 14 Sv of SPMW, about half of which recirculate within the subpolar

gyre, cross the Reykjanes Ridge and mainly join the East Greenland Current. Off Cape Farvel 13 Sv of SPMW and Arctic waters, passing through the Denmark Strait, are carried southwards. They are accompanied by 13 Sv of LSW below, including 3 Sv of recently formed LSW, which has not crossed the Reykjanes Ridge and recirculates in the Irminger Sea. In the bottom layer about 7 Sv of overflow waters are transported southwards along the Greenlandic continental slope, which are composed of 3 Sv of DSOW, 2 Sv of diluted ISOW, and 2 Sv of entrained SPMW. The major part of the 9 Sv of diluted ISOW entering the western Atlantic joins the Deep Northern Boundary Current in the Labrador Basin. East of the Reykjanes Ridge a balance of -7 Sv is established for the bottom layer, which leave the eastern Atlantic accompanied by 2 Sv of LDW (SM93). If the Iceland-Scotland Overflow is given by 3 Sv an entrainment of 4 Sv is required. 12 Sv of ISOW are transported southwards along the eastern flank of the Reykjanes Ridge. Of this about 3 to 5 Sv, depending on the dilution by LDW, must recirculate within the Iceland Basin or the West European Basin adjoining in the south. A cyclonic circulation of this magnitude is also suggested by Harvey and Theodorou (1986). All in all, about 15 Sv of bottom water have to be transported southwards in the Deep Western Boundary Current, including 3 Sv of LDW (SM93). Considering water with $\sigma_0 \geq 27.72$ kg/m³ the transport increases to 25 Sv if a formation rate of LSW of 7 Sv is assumed as in SM93, who arrived at a corresponding transport of 16 Sv. If about 18 Sv of North Atlantic Deep Water cross the equator (SM93), at least 7 Sv must upwell in the mid and low latitudes of the North Atlantic and recirculate to subpolar regions.

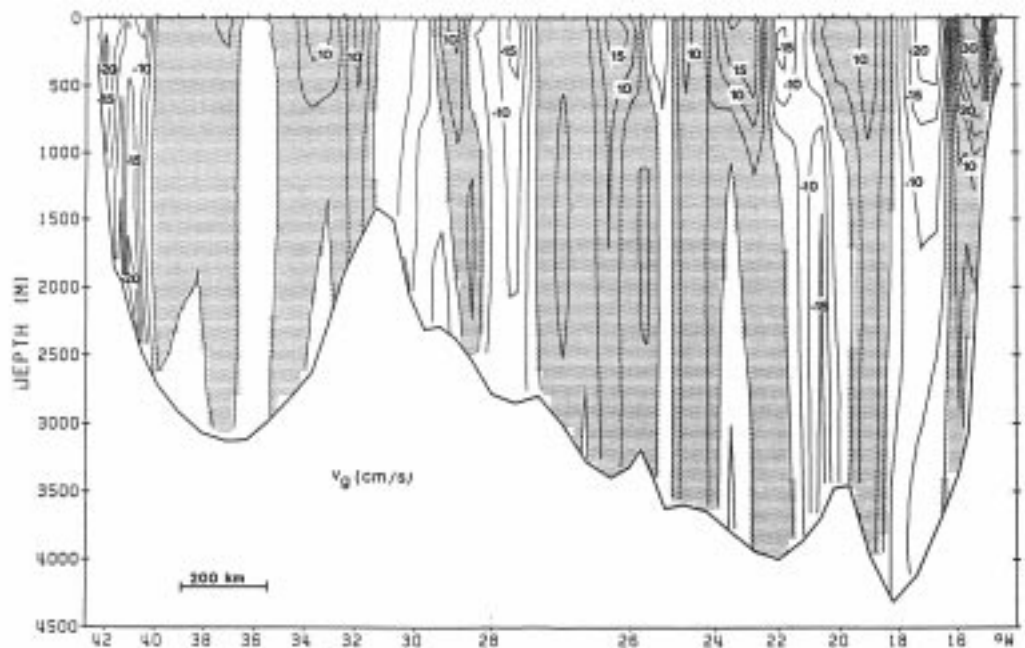


Figure 3. Vertical distribution of the geostrophic velocity adjusted to the corrected ADCP velocities along the Greenland-Ireland section.

Summary

All in all, the present transport scheme for the subpolar gyre of the North Atlantic supports that of SM93, though it tends to an intensified meridional circulation including an enhanced entrainment of SPMW into the lower layers and a larger transport of bottom water from the eastern to the western Atlantic. A reduced circulation of ISOW in the Irminger Basin and a recirculation of ISOW in the Iceland and West European basins are suggested.

References

- Clarke, R.A., 1984: Transport through the Cape Farewell–Flemish Cap section. *Rapp. P.-V. Reun. Cons. Int. Explor. Mer*, 185, 120–130.
- Gould, W.J., J. Loynes and J. Backhaus, 1985: Seasonality in slope current transports N.W. of Shetland. *Int. Counc. Explor. Sea*, CM 1985/C:7, Copenhagen, 6pp.

- Harvey, J.G., and A. Theodorou, 1986: The circulation of Norwegian Sea overflow water in the eastern North Atlantic. *Oceanologica Acta*, 9, 393–402.
- Krauss, W., 1986: The North Atlantic Current. *J. Geophys. Res.*, 91, 5061–5074.
- Schmitz, W.J., and M.S. McCartney, 1993: On the North Atlantic circulation. *Rev. Geophys.*, 31, 29–49.

ACSYS: The Arctic Climate System Study

Knut Aagaard, ACSYS SSG Chair, Applied Physics Laboratory, University of Washington HN-10, Seattle, WA 98195, USA

Background

Climate models generally suggest that global climate change will be amplified in the Arctic. Conversely, the Arctic has increasingly been assigned a significant role in global climate control, for example through its influence on the large-scale thermohaline circulation of the ocean and on the global heat budget (e.g., the snow and ice albedo feedback). However, neither the observational base, nor our knowledge of the controlling physical processes, nor our ability to model the role of the Arctic in global climate are presently sufficient to realistically assess the principal issues linking the Arctic with global climate.

In 1990, therefore, the Joint Scientific Committee (JSC) of the World Climate Research Programme (WCRP)

initiated an inquiry into the need for and feasibility of an Arctic Climate System Study under the WCRP. In 1992 the study group for this effort issued report WCRP-72 [Scientific Concept of the Arctic Climate System Study (ACSYS)], which suggested that an Arctic Climate System Study was now both timely and feasible. Shortly thereafter the JSC established the ACSYS project and appointed a scientific steering group that held its first meeting in fall 1992. The steering group has recently completed an initial implementation plan (WCRP-85, September 1994) and in November 1994 sponsored a conference in Gothenburg, Sweden on the dynamics of the arctic climate system. The proceedings will be published by the WCRP. The international project office for ACSYS has been established in Oslo, Norway, and a search is under way for the director of the office.

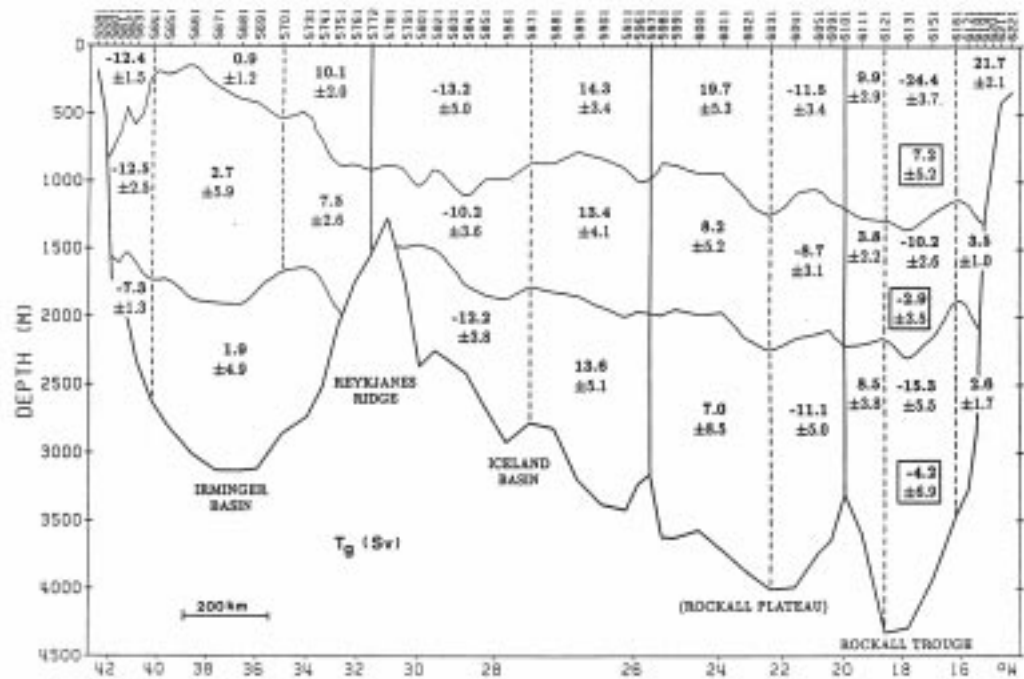


Figure 4. Vertical distribution of the volume transport in Sv across the Greenland-Ireland section. Negative values indicate southward transports. The three layers are separated by $\sigma_0 = 27.72 \text{ kg/m}^3$ and $\sigma_0 = 27.80 \text{ kg/m}^3$, respectively. Transports in the Rockall Trough are summed up for each layer and noted additionally.

The ACSYS goals and programme

The goal of ACSYS is to ascertain the role of the Arctic in global climate. To this end, ACSYS seeks to develop and coordinate national and international activities aimed at three primary objectives:

- (i) Providing a sound physical basis for an accurate representation of arctic processes in global climate models;
- (ii) Initiating long-term climate research and monitoring programmes for the Arctic; and
- (iii) Understanding the interactions between the Arctic Ocean circulation, the ice cover, and the hydrological cycle.

The implementation plan lays out a programme to assess the climatic role of the Arctic over the decade 1994–2004 by emphasizing five research topics:

- Ocean circulation (by an Arctic Ocean hydrographic survey, a set of shelf studies, an ocean variability project, and a historical data base project);
- Sea ice climatology (by establishing a sea ice data base, monitoring the export of ice through Fram Strait, and process studies);
- The arctic atmosphere (by process studies aimed at improved model parameterizations, re-analysis of the meteorological data base, and a polar clouds and radiation programme);
- The hydrological cycle (by compilation of an arctic hydrological data base, and by the development of selected regional hydrological models)
- Modelling (by developing a hierarchy of regional models, beginning with sea ice and continuing through coupled sea ice/ocean and atmosphere/sea ice/ocean models). Modelling also serves to integrate the other

research topics.

Efforts presently underway include historical data base assembly, ice thickness and export measurements, ocean variability studies, hydrographic mapping of the Arctic Ocean, a variety of modelling endeavours, and a start on studies of polar clouds and radiation.

Connections with WOCE

The ACSYS programme is meant to define the global climate role of a set of regionally connected processes in one of the global heat sinks (the north polar region), considering the atmosphere, the cryosphere, and the ocean together. The further intent is to deal with this complex interactive system in a region sufficiently small to be tractable within the ACSYS decade, but large enough to substantially describe a system relevant to global climate issues. The region chosen is that covered by the Arctic Ocean and its marginal seas. The connections between ACSYS and WOCE therefore relate both to regional issues and to processes. For example, ACSYS investigators expect to determine various fluxes from the Arctic Ocean into the North Atlantic sector of the World Ocean, including fluxes important to the thermohaline circulation such as salt and fresh water. In turn, ACSYS studies require the advective input of mass and heat to the Arctic from the seas to the south, where WOCE investigators are active. As another example, ACSYS investigators are extremely interested in shelf processes and in the means by which exchanges occur between the shelves and the adjacent deep ocean, including convecting plumes. A number of these process studies have considerable overlap with interests of WOCE investigators, both with respect to measurements and modelling.

WOCE DAC/SAC for Surface Meteorology Data and Surface Flux Analysis

David M. Legler, Center for Ocean-Atmospheric Prediction Studies, Florida State University, Tallahassee, FL 32306-3041, USA

A WOCE Data Assembly Center (DAC) for underway surface meteorological data is now established in the Center for Ocean-Atmospheric Prediction Studies at Florida State University (FSU) with support from the Oceanography Section, National Science Foundation (USA). This new centre accompanies a continuing Special Analysis Center (SAC) for derived air-sea fluxes.

The primary responsibility of the DAC is to collect, check, archive, and distribute all (underway) surface meteorology data from international WOCE vessels and moored buoys. These data typically include values for wind speed and direction, barometric pressure, humidity, air temperature, sea temperature, and in some installations, precipitation, and various radiation components. The frequency of measurements is typically once every several hours for the research vessel data, but there are also a

number of sophisticated instrument systems installed where values are automatically recorded once per minute. Some of these data have never been released to the research community in any form.

These data have many uses applicable to WOCE goals and programmes. Depending on the sampling frequency, ship location, and instruments involved, these data can be put to use in studies of mixed-layer variability, freshwater and heat budget analysis, validating remotely sensed data/products as well as ocean or atmospheric model results.

An example of some exciting data gathered for this project is data from the IMET systems (US WOCE Notes, Vol. 5(3)). A typical IMET system records one minute means of the standard variables mentioned previously including radiation measurements. There have been IMET

systems installed on several US platforms for WOCE investigations; RVs Knorr, Oceanus, Thompson and Melville, thus worldwide coverage is anticipated, including enhanced coverage of the Indian Ocean during 1995/96. Already processing is underway for data from the Knorr and Oceanus for years prior to 1995 (e.g. Fig.1). IMET data from moored platforms will also become part of the archives, e.g. the WOCE Subduction Experiment had four moored buoys equipped with IMET systems for the 2-year duration.

Data collection efforts for the DAC have begun in earnest. Already a number of data sets from various WOCE cruises have been transmitted to the DAC. However, these are but a small fraction of what should be available. Principal investigators responsible for surface meteorological data are encouraged to contact the DAC and submit data reports. The content and format for submitting data are detailed in the Hydrographic Programme Data Reporting manual (WOCE Publication 90-1). The surface meteorology DAC is extremely flexible and accepts nearly every form of data. There is often an incentive for the PIs to submit data; the DAC has previously taken datasets and returned improved/flagged datasets to the PIs.

The data will be quality controlled through a series of statistical and graphical analyses tools in order to pinpoint problems with the data, (e.g. spurious data, time shifts, gaps, biases, and instrument drifts) which will need to be

resolved with the upstream data supplier and/or flagged. Comparisons to other data sets will aid in qualifying this data for additional analysis.

The FSU SAC will continue toward its objective to provide and analyze fields *and uncertainty estimates* of surface fluxes of heat and momentum for tropical and mid-latitude oceans (60°N–60°S). These analyzed fields may serve as surface boundary conditions for numerical ocean models and validation tools for other flux products (e.g. those from numerical weather prediction centres such as ECMWF, NMC, JMA, etc.). All *in-situ* surface data will be used to provide monthly means of the flux fields; remotely-sensed data will be used to increase the spatial and temporal resolution of the fields. More details on SAC activities will be communicated in the future.

All DAC/SAC data products will be made accessible through a wide variety of distribution media (e.g. electronic network, magnetic, interactive requests, printed reports, etc.) to the WOCE community. Documentation (*i.e.* meta-data) regarding the observational data and the processing by the DAC likewise will be accumulated and distributed. Details of electronic contact information are given in the WOCE Data Handbook (available from the WOCE DIU). Already there is an FTP site for submitting or obtaining WOCE surface meteorology data (wocemet.fsu.edu) and soon there will be a WWW server installed for dissemination of data and information to WOCE community.

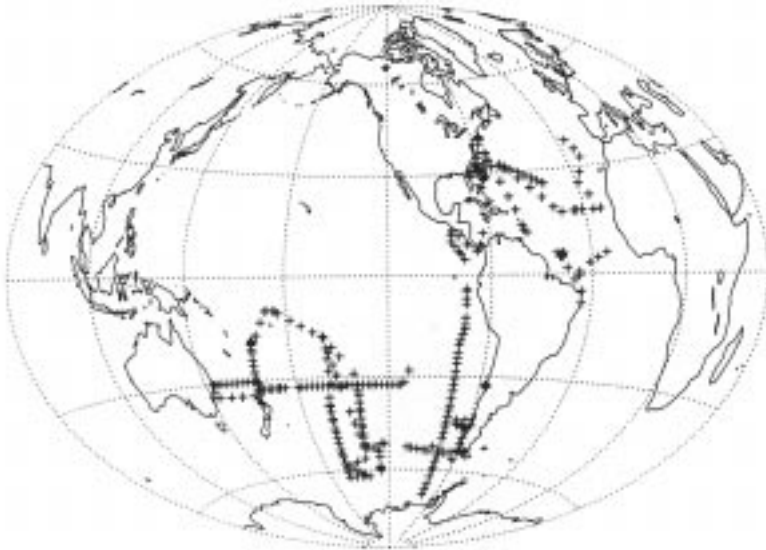


Figure 1. Locations of IMET data from the RV Knorr (WHOI) for the period May 1992-April 1994. Data are recorded once per minute during this period, but only the first position each day is indicated for clarity.

More information about the FSU DAC/SAC can be obtained by contacting the investigators:

David M. Legler &
James J. O'Brien
Center for Ocean-Atmospheric
Prediction Studies
Florida State University
Room 020 Love Bldg.
Tallahassee, FL 32306-3041
USA
Tel: 1-904- 644-4581
Fax: 1-904-644-4841
email: legler@coaps.fsu.edu,
obrien@coaps.fsu.edu

POP

Colourful images from the Parallel Ocean Processor Ocean Model (POP) are now available on the World Wide Web. To display them use MOSAIC or NETSCAPE. They may be reached via the WOCE IPO Home Page or by the command <http://vislab-www.nps.navy.mil/~braccio/>. We encourage other modellers to follow this example. It's a great opportunity to catch the attention of the WOCE community for your work.

A Consistent pre-WOCE Hydrographic Dataset for the South Atlantic: Station Data and Gridded Fields

V. Gouretski and K. Jancke, WHP Special Analysis Centre, Bundesamt für Seeschifffahrt und Hydrographie, 20359 Hamburg, Germany

Introduction

For many applications historical hydrographic data will be used together with the WOCE data. An *ad hoc* usage of historical data is often problematic, as they differ considerably in their accuracy due to changes over time in both instrumental techniques and requirements for the precision of measurements. Temperature remains the best measured parameter, while salinity and nutrient determinations still pose problems especially in the deep ocean with its weak gradients. A validation of the data quality is therefore an important stage of the data analysis. Usually results of the validation procedure are used to flag and reject erroneous or questionable data. Only few attempts are known to have been made to correct data. Speer and McCartney (1991) unbiased salinity of several cruises in the Atlantic Ocean by accounting for relative errors of the IAPSO Standard Sea Water, Mantyla (1994) treated salinity inconsistencies of modern and historical cruises in the eastern Atlantic and Reid (1994) used Mantyla's salinity corrections in his study of the circulation of the Atlantic Ocean.

High-quality hydrographic data showed a remarkable stability of the oceanographic parameters in some parts of the deep ocean. Saunders (1986) analyzing data from several cruises to the north-east Atlantic in 1980s came to the conclusion that "the uniformity of dissolved-oxygen concentration at the deepest level of the northeast Atlantic and uniformity of the potential temperature-salinity relationship there provide environmental standards against which measurements can be tested". The latter idea was used by Mantyla (1994) and is also applied here for the validation and adjustment of the South Atlantic historical data.

Evaluation of the accuracy of the historical salinity and oxygen data for the South Atlantic

We use the data from the Southern Ocean Data Base (SODB) of AWI, Bremerhaven, (Olbers *et al.*, 1992) to evaluate changes in the accuracy of salinity and oxygen measurements over the time period 1920 to 1991. The study area was divided into several boxes (Fig. 1) and θ -S and θ -O₂ scatter diagrams were constructed for each box. A proper range of potential temperature with linear θ -S and θ -O₂ relationships was selected for the deep part of the water column (minimum depth 1500 m). Within the selected ranges regressions of S and O₂ on θ were calculated along with standard deviations (σ_s, σ_o) from the

regression line. Table 1 presents results of this analysis for the decadal time periods between 1920 and 1991 in selected boxes. In each box a general decrease of σ_s, σ_o is evident and is explained by the general trend of increasing accuracy of salinity and oxygen measurements. The results are also shown for the refined and adjusted data described below (marked with asterix). Within each box standard deviations $\sigma_{s,o}$ were normalized by the reference standard deviation $\sigma_{s,o}$ (calculated from the refined and adjusted data for the time period 1970 to 1991). The ratios $r_{s,o} = \sigma_{s,o} / \sigma_{s,o}$ are used as a data quality indicator. Averaged over 12 boxes the ratios indicate an improvement of measurement precision by a factor of 5–6.

Data

The data originated from the following sources:

- (1) SODB data (3806 stations south of 30°S), (Olbers *et al.*, 1992);
- (2) part of J. Reid's collection (731 stations north of 30°S (Reid, 1989));
- (3) the bottle data from 360 stations of the South Atlantic Ventilation Experiment (SAVE).
- (4) the bottle data from 81 stations of the WOCE cruise A11.

The combined data set includes a total of 4978 stations (Fig. 1).

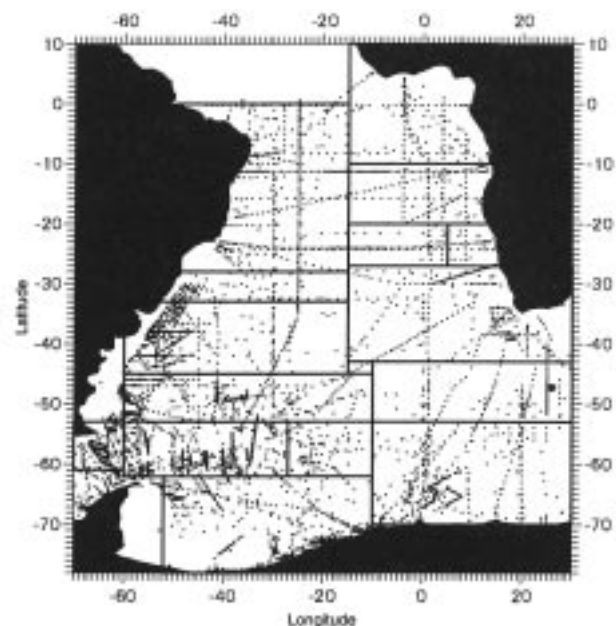


Figure 1. Station map of the consistent pre-WOCE hydrographic data set and boundaries of boxes used for quality control and adjustment of salinity and oxygen data.

In preparing our pre-WOCE South Atlantic data set we tried to select the data of higher quality and to achieve a certain degree of data consistency:

- (a) based on the quality analysis, data gathered before 1970 were generally rejected along with the data obtained aboard fishery vessels with their typically lower quality of salinity data. Some older data (15% of the total) were used to fill the data poor regions.
- (b) mostly full depth hydrographic casts were used (70% of the casts extend over at least 90% percent of the total depth at the station site).
- (c) all the data were subject to the same S, O_2 - θ diagram check.
- (d) an attempt was made to remove salinity and oxygen offsets between the stations on the basis of comparison with the deep water reference θ -S and θ - O_2 relationships.

The combined data set consists of hydrographic data of two types: bottle data (Nansen or CTD Rosette bottles), total of 4006 stations, and CTD 2-dbar resolution data (total of 972 stations). Data at the observed levels were linearly interpolated onto a set of 42 horizontal standard levels used in the atlas by Olbers *et al.* (1992). It is this interpolated data that were subject to the further validation, adjustment and gridding.

Validation of the data and treatment of salinity and oxygen inconsistencies

The quality evaluation of the combined data set was helped by the fact that all of the source data have already been validated to a certain degree. Thus, all SODB data were subject to a number of quality control checks described by Olbers *et al.* (1992) (range, static stability, standard deviation, vertical profile and scatter diagram checks along with a subjective control of raw maps). θ -S and θ - O_2 diagrams were used for the further refinement of the combined data set. Validation of the SODB data showed that a bad quality of the salinity measurements is not necessarily accompanied by a bad quality of the oxygen measurements. However while selecting the data we gave priority to the quality of salinity measurements.

For each sub-area shown in Fig. 1 a proper temperature range (an adjustment range) within the deep part of the water column (at least 1000 m deep) with a characteristic linear θ -S and θ - O_2 relations was chosen and regressions of S and O_2 on θ were calculated along with standard deviations (σ) of the observation points from the regression line. A subset of stations obtained after 1979 was used to calculate reference regressions.

The average offset of the salinity (oxygen) values within the adjustment θ -range from the reference regression line was then determined for each S, O_2 profile with at least 3 data points within the adjustment θ -range. After the removal of the individual offsets additional rejection of the 2.5- σ outliers was done. The treatment of the S, O_2 inconsistencies is based upon several assumptions:

Table 1. Change of salinity (S) and oxygen (O_2) precision over time in selected geographical boxes in the South Atlantic. Precisions are characterized by the normalized ratios r_s, r_o of the standard deviation (σ_s, σ_o) of observations from the regression line $S, O_2 = A_{s,o} \theta + B_{s,o}$ within a selected range of potential temperature θ . Only the data below 1500 m were used. Oxygen unit is ml/l.

Decade	σ_s	r_s	σ_o	r_o
Box [60-10°W 53-45°S] θ -range (°C) [-0.3 – 1.0]				
1920-29	0.0117	5.09	0.104	3.85
1930-39	0.0148	6.43	0.168	6.22
1950-59	0.0171	7.43	-	-
1960-69	0.0097	4.22	0.169	6.26
1970-79	0.0065	2.83	0.098	3.63
1980-93	0.0065	2.83	0.080	2.96
1970-93*	0.0023	1.00	0.027	1.00
1980-93*	0.0020	0.87	0.027	1.00
Box [15°W-30°E 43-27°S] θ -range [0.7 – 1.8]				
1920-29	0.0143	2.92	0.083	3.32
1930-39	0.0156	3.18	0.172	6.88
1950-59	0.0154	3.14	0.107	4.28
1960-69	0.0236	4.82	0.204	8.16
1970-79	0.0195	3.98	0.136	5.44
1980-93	0.0069	1.41	0.080	3.20
1970-93*	0.0049	1.00	0.025	1.00
1980-93*	0.0047	0.96	0.025	1.00
Box [10°W-30°E 70-53°S] θ -range [-0.7 – 0.2]				
1920-29	0.0087	4.14	0.057	1.30
1930-39	0.0063	3.00	0.113	2.57
1950-59	0.0236	11.24	0.109	2.48
1960-69	0.0121	5.76	0.124	2.82
1970-79	0.0103	4.90	0.116	2.64
1980-93	0.0061	2.90	0.166	3.77
1970-93*	0.0021	1.00	0.044	1.00
1980-93*	0.0019	0.90	0.040	0.91
Average over 12 boxes south of 30°S				
1920-29		3.99		1.87
1930-39		4.11		4.03
1950-59		6.08		1.21
1960-69		4.57		3.71
1970-79		3.41		2.73
1980-93		2.38		2.28
1970-93*		1.00		1.00
1980-93*		0.74		0.79

- (1) temperature is assumed to be measured perfectly;
- (2) temporal and spatial variability of the θ -S and θ - O_2 relationships within the box is neglected;
- (3) the S, O_2 offsets determined within the adjustment θ -range are assumed to be constant for the whole profile.

Objective analysis of the data

The validated and adjusted profile data were used to obtain a gridded data set by applying an optimal interpolation procedure (Gandin, 1963). The advantage of this method is that along with the estimator of the field a relative error

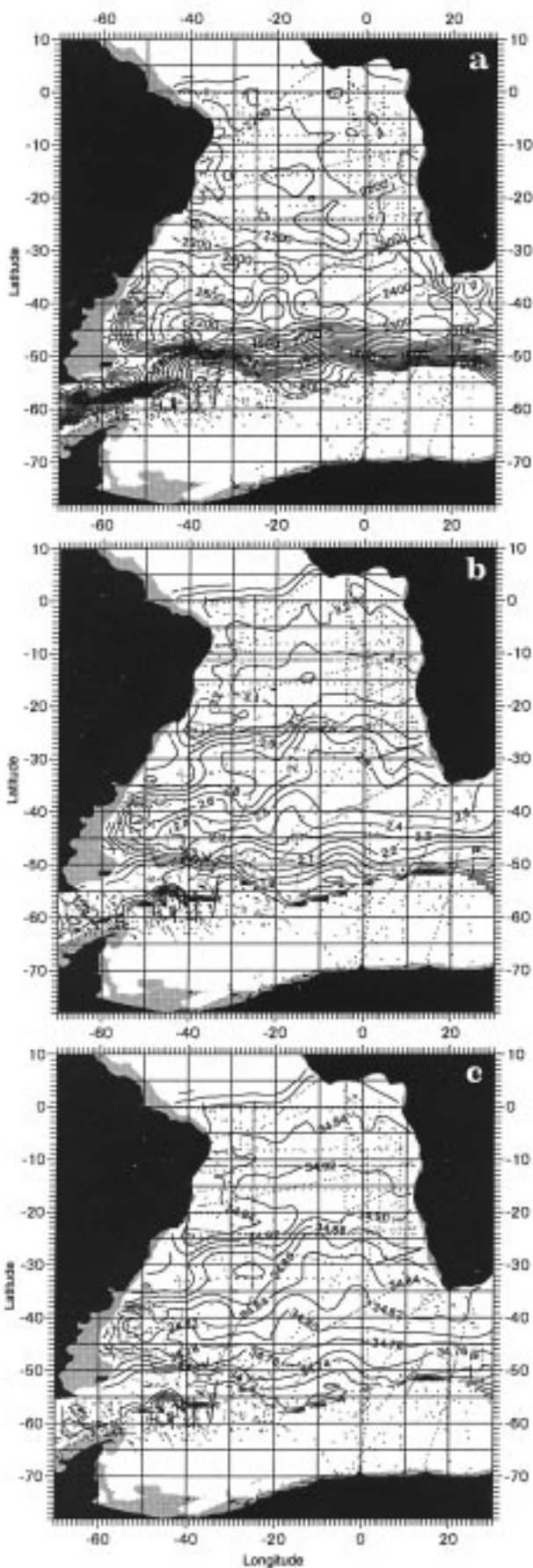


Figure 2. Properties of the isopycnal surface $\sigma_2 = 36.98 \text{ kg m}^{-3}$: (a) depth (m), (b) potential temperature ($^{\circ}\text{C}$), (c) salinity.

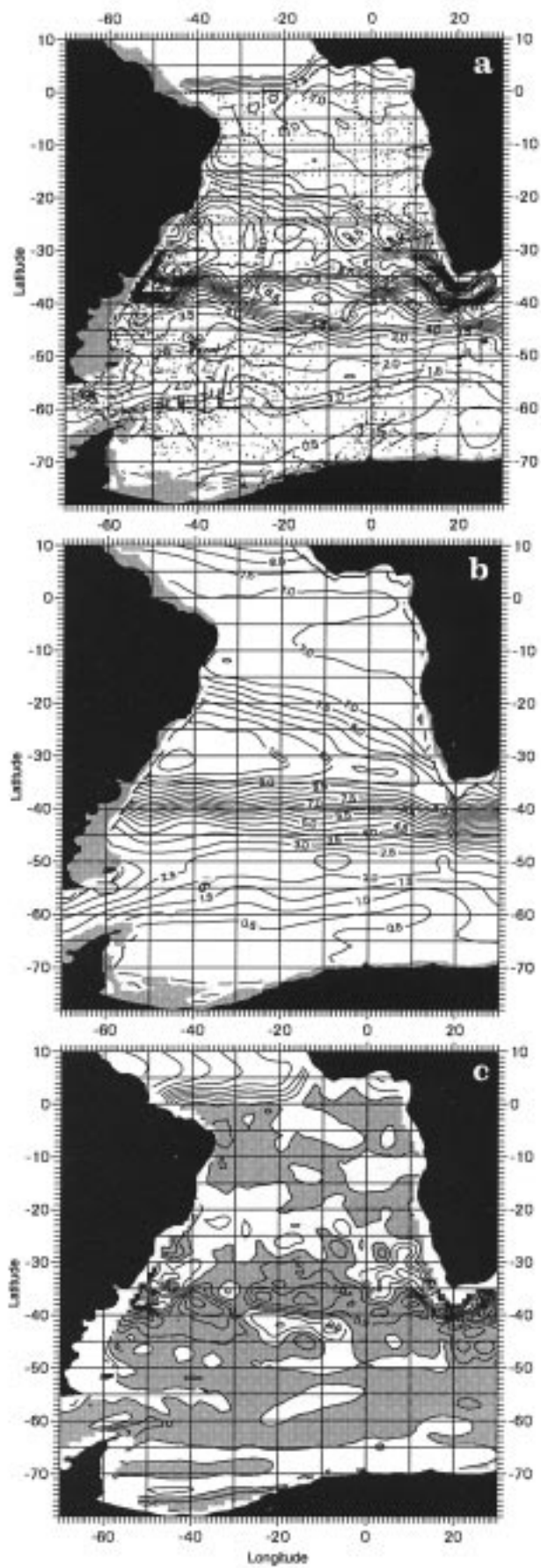


Figure 3. Climatological fields of potential temperature, ($^{\circ}\text{C}$) at 500 m: (a) present report, (b) Levitus et al. (1994), (c) difference (a)-(b).

variance is calculated. The optimal estimator of the field at the estimation point (x,y) is given by $F(x,y) = \sum a(x,y)_i f_i + M(x,y)$, where summation is over all observations f_i in the influence area and coefficients $a(x,y)$ are determined by the correlation structure of the observations. The quality of the method depends on the accuracy of the mean field $M(x,y)$, which was approximated by a linear regression of the data in both latitude and longitude. The numerical code is given courtesy of P. DeMey (DeMey and Menard, 1989).

The climatological fields were calculated for 39 standard levels between the surface and 5500 m and for a number of selected isopycnal surfaces (Reid, 1989). Shown in Fig. 2a-c are the properties of the isopycnal surface $\sigma_2 = 36.98 \text{ kg m}^{-3}$ which is a characteristic of the North Atlantic deep water as it spreads southwards in the South Atlantic Ocean.

Levitus *et al.* (1994) (further referred to as LBB) recently produced a new oceanographic atlas of the world ocean. A comparison of our and LBB climatology was done for an arbitrarily selected level of 500 m (Fig. 3a-c). A larger spatial averaging applied by LBB leads to the loss of some characteristic patterns such as strong gradients especially in the vicinity of the western boundary currents. Temperature differences between the two fields cover the range -4.3 to 2.9°C with the average standard deviation being 0.513°C . However, the average temperature difference is rather small (-0.07°C) implying a possibility to use LBB fields as a mean field $M(x,y)$ required by the objective analysis algorithm.

Data availability on the Internet

The analyzed fields and the profile data are ready for public access on the WHP SACs anonymous ftp server <ftp.dkrz.de>. The files are located in the directory `/pub/woce/Products/pre-WOCE/SouthAtlantic`, and stored in a compressed form. For further details see the ASCII file

WHP Manuals On-Line

Charles E. Corry, WOCE Hydrographic Programme Office, and Kai Jancke, WHP Special Analysis Centre

The WHP is making the relevant manuals of the WOCE program public through anonymous ftp. This service is provided in parallel to the distribution of printed copies of WOCE manuals by the WHP Special Analysis Center (SAC) in Hamburg. Available so far are updates and extensions to the WHPO 91-1 "Operations and Methods" manual, including the nutrients addition; Revision 2 of the Data Reporting manual, WHPO 90-1; and the NGDC manual for reporting bathymetric data, MGD77.

Manuals are stored both as PostScript and FrameMaker binary files in deflated form using zip compression routines that are also available from SAC. The NGDC MGD77

manually in that directory. They are accessible through ftp only, but to ease navigation the SAC WWW Home Page <http://www.dkrz.de/~u241046/>

Products will lead to the data as well. Full details of the preparation of the data set are given in the SAC Technical Report No. 1 (WOCE Report No. 127/95) in `/pub/woce/Reports/SAC-01.zip`.

References

- Gandin, L.S., 1963: Objective Analysis of the meteorological fields. Leningrad, Gidrometeoizdat, 287pp. (In Russian) (English translation No. 1373 by Israel Program for Scientific Translations (1965), Jerusalem, 242pp.)
- Levitus, S., R. Bugget and T.P. Boyer, 1994: World Ocean Atlas 1994. Volume 3: Salinity. NOAA Atlas NESDIS 3, 99pp.
- Mantyla, A.W., 1994: The treatment of inconsistencies in Atlantic deep water salinity data. *Deep-Sea Res.*, 41, 1387-1405.
- DeMey, P., and Y. Menard, 1989: Synoptic analysis and dynamical adjustment of GEOS-3 and SEASAT altimeter eddy fields in the North West Atlantic. *J. Geophys. Res.*, 94, 6221-6231.
- Olbers, D., V.V. Gouretski, G. Seiss and J. Schroeter, 1992: Hydrographic Atlas of the Southern Ocean. Alfred-Wegener-Institut, Bremerhaven, 17pp., 82 plates.
- Reid, J.L., 1989: On the total geostrophic circulation of the South Atlantic Ocean: Flow patterns, tracers, and transports. *Prog. in Oceanogr.*, 23, 149-244.
- Reid, J.L., 1994: On the total geostrophic circulation of the North Atlantic Ocean: flow patterns, tracers, and transports. *Prog. in Oceanogr.*, 33, 1-92.
- Saunders, P.M., 1986: The accuracy of measurement of salinity, oxygen, and temperature in the deep ocean. *J. Phys. Oceanogr.*, 16, 189-195.
- Speer, K.G., and M.S. McCartney, 1991: Tracing lower North Atlantic deep water across the equator. *J. Geophys. Res.*, 96, 20, 443-20, 448.

manual is only available as a zipped plain-text file, however.

Inflated PostScript files will print on both A4 and US letter sized paper, though occasionally some text may be cut off on US letter paper. Insuring that the page size is set to A4 in your "Page Setup", even though you are using US letter paper should minimize that, however. The manuals will print duplex (double sided) if you have a duplex-capable printer, or single sided on most PostScript printers.

For those users with FrameMaker 4.0.x, binary files are provided. FrameMaker files can also be opened and printed using FrameViewer 4.0.x available for \$50 US (retail) or \$25 US (educational) from:

Frame Technology Corp.
1010 Rincon Circle
San Jose, CA 95131, USA
Outside sales: Gretchen Wirth
Telephone: 408-428-6109
Internet: gwirth@frame.com

Note that FrameMaker or FrameViewer require Windows on PCs with at least 8 MB of RAM and, while they will run on a 386, performance is much better on a 486. On a Macintosh at least 5 MB of RAM are required. Unix versions are also available.

After unzipping, on at least some Unix platforms the access/ownership bits are all cleared, and it may be necessary to change mode (chmod) before the unzipped files are usable.

Users unable to access or print the electronic versions and who need paper copies should contact either Kai Jancke (kai.jancke@m5.hamburg.bsh.d400.de) or Chuck Corry (ccorry@whoi.edu). If you have received WHP manuals from us in the past you will automatically be sent these manuals when they are printed and you do not need to contact us. At present we expect the printed manuals to be available in February 1995.

Uncompression, or unzip software for a variety of machines, e.g., MS DOS PC, Macintosh, Unix workstations, and VAX/VMS are provided as well for those users who do not already have the zip utility, or whose present version does not correctly unzip the files. Users experiencing difficulties with these utilities or the electronic versions of the manuals should contact Kai Jancke. The most common problem users have encountered has been with the use of incompatible zip programs. Thus, we recommend that you obtain the SAC versions of the zip utility for your machine

before trying to unzip any of the available manuals or data.

How to get these Files:

The files are provided through anonymous ftp from ftp.dkrz.de (136.172.110.11) login name is either "ftp" or "anonymous", the password is your e-mail address. If your ftp program stops unexpectedly, please try again with a "-" (minus sign) in front of the password.

Note that after login the case of the letters is significant!!!

After logging in change directories to /pub/woce/Manuals. The ASCII file OReadme gives an overview of the file contents in this directory. The updates and additions to WHPO 91-1 are in the /Operations.and.Methods subdirectory. Revision 2 of WHPO 90-1 and the bathymetric manual, MGD77, are in subdirectory /Data.Reporting. Further instructions for obtaining the available WOCE hydrographic data from SAC are given in the data reporting manual WHPO 90-1.

All files ending with .ZIP in the name ***must*** be transferred in binary mode or the unzipping will fail! PC and VAX users will need to rename the files to conform to DOS or VMS usage (8 character file name, 3 character extension). Use a variation of the get, or mget, command to do this on retrieval, for example, "get 91-1.nuts.zip nuts.zip", where "nuts.zip" is the file name to be used on your machine and "91-1.nuts.zip" is the name of the file on the ftp server. If using Frame files please insure the file extension for the unzipped files is .DOC if you are working in an MS-Windows environment.

Unzipping programs for decompression are found in the /pub/woce/util/executables directory.

A Note on Data Sharing Policy

In the November 1994 issue you carried an article by Dale Pillsbury and a note from Bob Dickson, both on the subject of WOCE Current Meter records. Dale remarks that data has been slow to arrive at the Current meter DAC and Bob's note suggests there are 1500 WOCE records (cm years?) available. Both the DAC operation and Bob's compilation respect the PI's "rights" by restricting publication to the basic statistics until a date agreed with the PI so there appears to be little reason, if the statistics are available, not to deposit the actual records in the WOCE DAC. The WOCE data sharing policy for moorings recommends that the PI should make the data public two years after recovery of the final deployment at a site. In developing WOCE, we envisaged that:

- (a) the statistics could be available soon after each deployment,
- (b) that the data would be lodged (with security flags) with the DAC as soon as the PI was reasonably happy with the data,
- (c) that this would allow the DAC to do an independent quality control of the data and report back to the PI (much like the DQE effort in the WHP, except that the DAC would do it in-house).

There is NO evidence of abuse of PI priorities in any of the DACs so I urge the PIs to collaborate with the DAC in its efforts to assemble the global set of current observations envisioned in the planning of WOCE.

Jim Crease, WOCE DIU

WOCE IPO Publications Since the Start of 1994

- 111/94 WOCE INTERNATIONAL PROJECT OFFICE
1994 Report of the sixth meeting of the WOCE/
TOGA Surface Velocity Programme Planning
Committee, SVP-6, Honolulu, HI, USA, 28–30
September 1993. 38pp.
- 112/94 WOCE INTERNATIONAL PROJECT OFFICE
1994 WOCE Numerical Experimentation Group
Science Plan for Ocean Modelling 1993: WOCE
strategy for ocean modelling. 35pp.
- 113/94 WOCE INTERNATIONAL PROJECT OFFICE
1994 Report of the sixth meeting of the WOCE Data
Management Committee, DMC-6, University of
Colorado, Boulder, CO, USA, 1–2 December 1993.
21pp.
- 114/94 WOCE INTERNATIONAL PROJECT OFFICE
1994 Report of the twelfth meeting of the WOCE
Hydrographic Programme Planning Committee,
WHP-12, Woods Hole Oceanographic Institution,
Woods Hole, MA, USA, 8–10 September 1993.
16pp.
- 115/94 WOCE INTERNATIONAL PROJECT OFFICE
1994 Report of the sixth meeting of the WOCE Core
Project 1 Working Group, CP1-6, Institut für
Meereskunde, Kiel, Germany, 30 August–1
September 1993. 23pp.
- 116/94 WOCE INTERNATIONAL PROJECT OFFICE
1994 Report of the twentieth meeting of the JSC
WOCE Scientific Steering Group, WOCE-20,
Takebashi Kaikan, Tokyo, Japan, 9–11 November
1993. 27pp.
- 117/94 WOCE INTERNATIONAL PROJECT OFFICE
1994 WOCE Numerical Experimentation Group:
Report of the Eighth Meeting (NEG-8) and Workshop
on Ocean Models for Climate Research, Institute of
Ocean Sciences, Vancouver Island, Canada, 13–15
September 1993. 33pp.
- 118/94 WOCE INTERNATIONAL PROJECT OFFICE
1994 The WOCE Handbook, 5th edition: A guide
to WOCE scientific infrastructure for 1994. 44pp.
- 119/94 WOCE INTERNATIONAL PROJECT OFFICE
1994 Summary and Assessment of Resource
Commitments. 64pp.
- 120/94 WOCE DATA INFORMATION UNIT 1994 WOCE
Data Handbook. (Second Printing) 180pp. Looseleaf.
- 121/94 WOCE INTERNATIONAL PROJECT OFFICE
1994 Report of the third meeting of the TOGA/
WOCE XBT/XCTD Programme Planning
Committee (TWXXPPC-3) and Report of the fifth
meeting of the WOCE Upper Ocean Thermal Data
Assembly Centres Coordination Group (UOT/DAC-
5), RSMAS, University of Miami, Miami, FL, USA,
25–29 April 1994. 36pp.
- 122/94 WOCE INTERNATIONAL PROJECT OFFICE
1994 Report of the WOCE Hydrographic Programme
Data Meeting, US National Science Foundation,
Arlington, VA, USA, 24–25 May 1994. 23pp.
- 123/95 WOCE INTERNATIONAL PROJECT OFFICE
1995 Report of the twenty-first meeting of the
WOCE Scientific Steering Group, WOCE-21, Institut
für Meereskunde, Universität Kiel, Germany, 12–14
October 1994. 31pp.
- 124/95 WOCE INTERNATIONAL PROJECT OFFICE
1995 Report of the seventh meeting of the WOCE
Data Products Committee, DPC-7, James Rennell
Centre for Ocean Circulation, Southampton, UK,
13–15 September 1994. 22pp.
- 125/95 WOCE INTERNATIONAL PROJECT OFFICE
1995 Report of the Ninth Meeting of the WOCE
Numerical Experimentation Group (NEG-9) and 1994
Workshop, Los Alamos National Laboratory, NM,
USA, 19–21 September 1994. 24pp.
- 126/95 WOCE INTERNATIONAL PROJECT OFFICE
1995 Overview of WOCE Activities: WHP –
Moored Arrays – Floats – Drifters – XBTs – Sea
Level – Satellites – Modelling – Data Information –
Facilities. 55pp.
- 127/95 WOCE HYDROGRAPHIC PROGRAMME
SPECIAL ANALYSIS CENTRE 1995 Gouretski,
V., and K. Jancke. A Consistent pre-WOCE
Hydrographic Data Set for the South Atlantic: Station
Data and Gridded Fields. WHP SAC Technical
Report No. 1.
- 128/95 WOCE INTERNATIONAL PROJECT OFFICE
1995 Report of the thirteenth meeting of the WOCE
Hydrographic Programme Planning Committee
(WHP-13), College of Marine Sciences, National
Sun Yat-Sen University, Kaohsiung, Taiwan, ROC,
2–4 November 1994. 23pp.
- 129/95 WOCE INTERNATIONAL PROJECT OFFICE
1995 Report of the Seventh Meeting of the WOCE/
TOGA Surface Velocity Programme Planning
Committee (SVP-7), Sea Lodge at La Jolla Shores,
CA, USA, 2–4 November 1994. 31pp.

Note on Copyright

Permission to use any scientific material (text as well as figures) published in the International WOCE Newsletter should be obtained from the authors.

Meeting Timetable

WOCE Meetings

April	24–28 1995	DPC-8	Tallahassee, FL
May	2–5 1995	UOT-DAC QC Workshop	La Jolla, CA
June	8–9 1995	IWP-3	Paris

Science and other Meetings

April	2–7 1995	International TOGA Science Conference, Melbourne
April	3–7 1995	European Geophysical Society XX General Assembly, Hamburg
April	18–21 1995	The Oceanographic Society: Fourth Scientific Meeting, Newport, Rhode Is.
	May 29–June 2 1995	29th Annual Congress of the Canadian Meteorological and Oceanographic Society, Kelowna, BC
June	5–12 1995	XVIII Pacific Science Congress, Beijing
June	12–16 1995	CLIVAR SSG-4, Hamburg
June	13–27 1995	IOC Assembly, Paris
June	26–29 1995	The Seas of Southeast Asia – the Key to Regional Climate Patterns, Lombok
July	2–14 1995	IUGG XXI General Assembly, Boulder
August	5–12 1995	IAPSO XXI General Assembly, Honolulu
September	4–8 1995	3rd International Conference on Modelling of Global Climate Change and Variability, Hamburg
September	25–29 1995	IGBP – Global Analyses Interpretation and Modelling, Garmisch

For more information on the above meetings contact the IPO.

If you are aware of any conferences or workshops which are suitable for the presentation of WOCE results and are not mentioned in the above list please let the IPO know.

WOCE is a component of the World Climate Research Programme (WCRP), which was established by WMO and ICSU, and is carried out in association with IOC and SCOR. The scientific planning and development of WOCE is under the guidance of the JSC Scientific Steering Group for WOCE, assisted by the WOCE International Project Office. JSC is the main body of WMO-ICSU-IOC, formulating overall WCRP scientific concepts.

The WOCE Newsletter is edited at the WOCE IPO at the Institute of Oceanographic Sciences Deacon Laboratory, Brook Road, Wormley, Godalming, Surrey, GU8 5UB, UK (Tel: 44-1428-684141, Fax: 44-1428-683066, e-mail: woceipo@unixa.nerc-wormley.ac.uk). Financial support is provided by the Natural Environment Research Council, UK.

Scientific material should not be used without agreement of the author.

We hope that colleagues will see this Newsletter as a means of reporting work in progress related to the Goals of WOCE as described in the Scientific Plan. The SSG will use it also to report progress of working groups, experiment design and models.

The editor will be pleased to send copies of the Newsletter to institutes and research scientists with an interest in WOCE or related research.